NAVAL POSTGRADUATE SCHOOL
Monterey, California

THESIS

RIP CURRENT SPACING IN RELATION TO WAVE ENERGETICS AND DIRECTIONAL SPREADING

by

Robert D. Holt

June 2003

Thesis Advisor:	Edward Thornton
Second Reader:	Timothy Stanton

THIS PAGE INTENTIONALLY LEFT BLANK

REPORT DOCUMENTATION PAGE			Form Approved OMB No. 0704-0188
Public reporting burden for this collection of information is estimated to average 1 hour per response, including the time for reviewing instruction, searching existing data sources, gathering and maintaining the data needed, and completing and reviewing the collection of information. Send comments regarding this burden estimate or any other aspect of this collection of information, including suggestions for reducing this burden, to Washington headquarters Services, Directorate for Information Operations and Reports, 1215 Jefferson Davis Highway, Suite 1204, Arlington, VA 22202-4302, and to the Office of Management and Budget, Paperwork Reduction Project (0704-0188) Washington DC 20503.			
1. AGENCY USE ONLY *(Leave blank)*	**2. REPORT DATE** JUNE 2003	**3. REPORT TYPE AND DATES COVERED** Master's Thesis	
4. TITLE AND SUBTITLE: Title (Mix case letters) Rip Current Spacing in Relation to Wave Energetics and Directional Spreading			**5. FUNDING NUMBERS**
6. AUTHOR(S) Holt, Robert D.			
7. PERFORMING ORGANIZATION NAME(S) AND ADDRESS(ES) Naval Postgraduate School Monterey, CA 93943-5000			**8. PERFORMING ORGANIZATION REPORT NUMBER**
9. SPONSORING /MONITORING AGENCY NAME(S) AND ADDRESS(ES) N/A			**10. SPONSORING/MONITORING AGENCY REPORT NUMBER**
11. SUPPLEMENTARY NOTES The views expressed in this thesis are those of the author and do not reflect the official policy or position of the Department of Defense or the U.S. Government.			
12a. DISTRIBUTION / AVAILABILITY STATEMENT Approved for public release; distribution is unlimited.			**12b. DISTRIBUTION CODE**

13. ABSTRACT ***(maximum 200 words)***

Rip current spacings are compared with wave energetics and directional spreading in the Southern Monterey Bay. Southern Monterey Bay affords a unique environment to study rip currents owing to their prevalence created by near-normally incident waves on a sandy shoreline. It is hypothesized that rip current spacing is a function of wave directional spreading and energy flux, based on the morphodynamic modeling by Reniers *et al.* 2003. A gradient of wave energy flux exists due to headlands and refraction over Monterey Canyon. Rip currents are shown to occur between cusps in the shoreline, allowing cusp spacing to be a surrogate for rip spacing. Rip current spacing was inferred from beach morphology surveys, LIDAR imagery, and Argus cameras, and found to be O(150m) at Sand City and O(300m) at Marina, separated by $\square 6km$. Measured waves during a two month period using wave-rider buoys, show a gradient of across-shore energy flux between Sand City, $\overline{F}_x \cong 28000(J/m^2)$, and Marina, $\overline{F}_x \cong 33000(J/m^2)$. The two sites have the same peak directional spreading of energy value, $\sigma_{peak}=14^\circ$, and slightly different bulk values for Sand City, $\sigma_{bulk}=18^\circ$, and Marina, $\sigma_{bulk}=20^\circ$. Therefore, the variations in rip current spacing could not be attributed to directional spreading but appear related to variations in energy flux.

14. SUBJECT TERMS Oceanography, Nearshore, Rip Currents, Directional Spreading, Beach Cusps, Coastal Video Imaging			**15. NUMBER OF PAGES** 79
			16. PRICE CODE
17. SECURITY CLASSIFICATION OF REPORT Unclassified	**18. SECURITY CLASSIFICATION OF THIS PAGE** Unclassified	**19. SECURITY CLASSIFICATION OF ABSTRACT** Unclassified	**20. LIMITATION OF ABSTRACT** UL

NSN 7540-01-280-5500 Standard Form 298 (Rev. 2-89)
Prescribed by ANSI Std. 239-18

THIS PAGE INTENTIONALLY LEFT BLANK

Approved for public release; distribution is unlimited.

RIP CURRENT SPACING IN RELATION TO WAVE ENERGETICS AND DIRECTIONAL SPREADING

Robert D. Holt
Ensign, United States Navy Reserve
B.S., United States Naval Academy, 2002

Submitted in partial fulfillment of the
requirements for the degree of

MASTER OF SCIENCE IN PHYSICAL OCEANOGRAPHY

from the

NAVAL POSTGRADUATE SCHOOL
June 2003

Author: Robert D. Holt

Approved by: Edward B. Thornton
Thesis Advisor

Timothy Stanton
Second Reader/Co-Advisor

Mary Batteen
Chairman, Department of Oceanography

THIS PAGE INTENTIONALLY LEFT BLANK

ABSTRACT

Rip current spacings are compared with wave energetics and directional spreading in the Southern Monterey Bay. Southern Monterey Bay affords a unique environment to study rip currents owing to their prevalence created by near-normally incident waves on a sandy shoreline. It is hypothesized that rip current spacing is a function of wave directional spreading and energy flux, based on the morphodynamic modeling by Reniers *et al.* 2003. A gradient of wave energy flux exists due to headlands and refraction over Monterey Canyon. Rip currents are shown to occur between cusps in the shoreline, allowing cusp spacing to be a surrogate for rip spacing. Rip current spacing was inferred from beach morphology surveys, LIDAR imagery, and Argus cameras, and found to be O(150m) at Sand City and O(300m) at Marina, separated by $\sim 6km$. Measured waves during a two month period using wave-rider buoys, show a gradient of across-shore energy flux between Sand City, $\overline{F}_x \cong 28000(J/m^2)$, and Marina, $\overline{F}_x \cong 33000(J/m^2)$. The two sites have the same peak directional spreading of energy value, $\sigma_{peak} = 14^\circ$, and slightly different bulk values for Sand City, $\sigma_{bulk} = 18^\circ$, and Marina, $\sigma_{bulk} = 20^\circ$. Therefore, the variations in rip current spacing could not be attributed to directional spreading, but appear related to variations in energy flux.

THIS PAGE INTENTIONALLY LEFT BLANK

TABLE OF CONTENTS

THIS PAGE INTENTIONALLY LEFT BLANK

LIST OF FIGURES

THIS PAGE INTENTIONALLY LEFT BLANK

ACKNOWLEDGMENTS

For infusing me with a passion for the nearshore and its no longer mysterious undercurrents, I thank Professor Thornton. Enough beach surveys in the past year have given me a mighty respect for rip currents and gradients of wave energy along a coast.

For opening my mind to the importance of turbulence, both great and small, throughout the ocean, and for never letting me doubt the validity and contribution of this project to the nearshore community, I thank Professor Stanton.

For serving as my MATLAB Rosetta Stones, I sincerely thank several folks: Mark Orzech, Rob Wyland, Paul Jessen, and Jim Stockel. Gentleman, you saved my wrists from Carpal Tunnel and my mind from spontaneous implosion. I cannot thank you enough for your expertise with coding and your patience to hear out my inept questions on the subject.

Jamie, Ad, and Denis, you three have my gratitude for being the most relaxed Post-Docs. I have ever had the pleasure to meet. You made the office a joy to work in.

To my friends and classmates, without your supreme patience, especially during the last few months, I do believe I would have a few gray hairs by now. Your support for my concurrent sleep-deprivation experiment is much appreciated.

A final call goes to my family. Growing up, I never imagined that I could earn a degree in "tide-pool stomping." Little did I know…Thank you for instilling me with a love for all things aquatic, and for your faith in letting me dive into the deeps to see how far I might go.

THIS PAGE INTENTIONALLY LEFT BLANK

I. INTRODUCTION

A. RIP CURRENTS

Rip currents are perhaps the most visible feature in the nearshore, in terms of scientific interest and public awareness. They are strong, jet-like currents that flow seaward across the surf zone in narrow channels, carrying with them sediment up to several surf zone widths offshore (Huntley and Short 1992). They are easily distinguished by "zones of roiled water and foam," (Shepard 1936) typically discolored, moving offshore and interfering with the incoming waves. Their occurrence is generally regulated to intermediate beaches, with reflective and dissipative beaches exhibiting little rip activity (Short 1985). Rip currents are an important nearshore process responsible for offshore sediment transport, beach erosion and accretion, rapid variations in coastal morphology, pollution transport, and hazardous swimming conditions (Huntley and Short 1992; Ranasinghe *et al.* 2001).

Early rip current research stemmed from a need to differentiate them from the "undertow" and "riptides" that plagued swimmers and exhausted lifeguards at Venice Beach, CA (Shepard 1936). Efforts were made to study their nature and morphological importance (Shepard, Emery and La Fond 1941). Initial studies were either qualitative or crude in their experimental setup, often-employing dyes, surface floats (drift bottles), and hours of visual observation (Shepard and Inman 1950). Early investigators concluded that a relationship existed between the spacing of the rips and the incident angle and groupiness of the incoming wave trains.

Several theories and empirical equations have been proposed to account for the regularity and persistence of rip current spacing. All the theories are based on alongshore and cross-shore spatial and temporal variations of radiation stress. The setup of the waves in the surfzone does not completely balance the incoming radiation stress generated by the waves; therefore, currents are generated in the surfzone to return this water offshore (Longuet-Higgins and Stewart 1964). In nearshore circulation cells, such as rip systems, this water will flow downward from regions of high waves (high setup) as

feeder currents into the low wave regions where it is returned offshore as a rip current (Dalrymple 1975).

The rip current theories vary by the cause of the alongshore variations in the radiation stress. Bowen and Inman (1969) showed that in theory and the laboratory for a planar beach that that there is a coupling between an incident wave train and a standing edge wave that results in a longshore variation in wave height and radiation stress. This in turn results in preferential spacing for the rip currents at alternating antinodes of the sub-harmonic standing edge waves of mode n=0. However, this rather special scenario is seldom observed in nature.

Bowen (1969) considered the case of a normally incident uniform wave train on a beach with undulating bottom topography. Alongshore variation of radiation stresses are created by waves refracting over the undulating bathymetry, from which Bowen obtained an analytical solution by linearizing the equations of motion. Circulation cells were alculated in which shoreward and offshore flows were of equal streamline spacing.

Sonu (1972) found that rip current cells were observed with O(60m) spacing at a Florida coast for a smooth beach with normally incident waves. The waves tended to break in the depressions vice the shoals, in contrast with observations by Shepard (1950) off of Scripps Beach. Sonu (1972) considered the cases for alongshore variations in radiation stresses due to alongshore variations in wave height offshore and uniform waves incident upon an undulating bathymetry. Either leads to the generation of nearshore circulation cells.

Alongshore varying wave momentum flux was generated by Dalrymple (1975) using intersecting wave trains. Dalrymple (1975) showed in theory and laboratory, that intersecting waves of opposite direction but of the same period generated alongshore-varying radiation stresses and a stationary rip system. Fowler and Dalrymple (1990) generalized Dalrymple (1975) by considering two groups of directionally narrow random waves of opposite but different directions, which resulted in a slowly propagating rip current system.

Most recently, Reniers *et al.* (2003b) generalized the work by Fowler and Dalrymple (1990) by considering a directionally broad energy spectrum at the offshore boundary applied to the non-linear shallow water equations. They show that the groups of incident waves arrive at the shoreline with alongshore length scales comparable to the rip spacing. The spatially variable energy generates variable radiation stresses that create low frequency (~15min period) vortices with alongshore length scales that act to perturb the initially alongshore-uniform bathymetry. A positive feedback of the forced vortices with the perturbed bathymetry results in an alongshore bar incised by rip channels. The spacing is related to the directional spreading and energy of the incoming wave train (Figure 1).

B. BEACH CUSPS

Rarely is a shoreline longshore uniform. More commonly, due to the complex interaction of the waves, currents, and local topography, a coastline is three-dimensional and exhibits a variety of features such as offshore bars, rip current cells, and beach cusps. Cuspate features ranging from O(10m) meter spacing on dissipative beaches with low wave energy to O(10,000) meter spacing in the case of the North Carolinian capes are prevalent on many beaches (Komar 1998). This study focuses on what are known in the literature as "rhythmic topography," "sand waves," or "giant cusps," (1998), (as opposed to beach cusps, O(10m)), of O(100) spacing that characterize the Southern Monterey Bay shoreline and will be referred to simply as cusps for this study (Figure 2).

The dynamics between beach cusps of various sizes and rip currents is not well understood, though they have been documented since the inception of rip current research (Shepard, Emery and La Fond 1941). Rip currents were found to exist in the embayments of both small and larger cuspate formations of Scripps Beach. In contrast, observations by Komar (1971) in the field and the laboratory indicated that the rips emerged from the shoals. This is consistent with the relationship between breaking wave height and depth found by Mei and Liu (1976), *i.e.* rhythmic bathymetric contours in the nearshore would force the rip from the embayments into the shoals. However, the relatively small width of the rip channels compared to the shoals negates the radiation

stress imbalance caused by the later wave breaking in the embayments. Consequently, rip channels form within the embayments, not the shoals.

Southern Monterey Bay affords a unique environment for the study of rip currents owing to their prevalence created by near normally incident waves impinging on a sandy shoreline. Sheltered by headlands to the north and the south, the predominant Pacific NW swell from the Aleutians enters the bay as a narrow-banded wave train (Munk and Traylor 1947; MacMahan *et al.* 2002b). The strong refraction over the Monterey Bay Canyon tends to bend the wave trains into a near normal approach to the shoreline. This refraction also leads to dramatic gradients in wave energy from the sheltered barred beach of Del Monte to the energetic, rip-dominated shore of Marina State Park (Figure 3). It is hypothesized that the spacing of the rip current channels is related to the directional spreading of the incoming wave trains.

Given the difficulties of making in situ nearshore bathymetric measurements, it will first be shown that for a cuspate shoreline in the Southern Monterey Bay, there is a rip in the center of each cusp. Evidence for the relationship between rip currents and embayments in the Southern Monterey Bay is demonstrated in the aerial photograph from 1984 (Figure 4). Taken on an energetic day at low tide with the sun directly overhead, the photo clearly shows rips to be located in the center of each cuspidal embayment. Therefore, the more easily measured cusp spacing will be used as a surrogate for rip spacing. Beach cusp formation favors normally incident wave trains (Longuet-Higgins and Parkins 1962). Given the prevalence of normally incident waves along Southern Monterey Bay, cusps and embayments are rhythmic features common to this study area. The image only covers a small portion of the coastline, but is representative of the Southern Monterey Bay from Sand City until the Salinas River. In the next section, the determination of rip current morphology by in situ surveys and remote sensing using LIDAR and video imaging (Argus) is described. The wave climate is then described, followed by how the rip current spacing is related to the wave climate.

II. RIP CURRENT MORPHOLOGY

A. SURVEYS

A study of coastal morphology must be able to account for rapid changes in bathymetry and beach morphology over a range of wave conditions, and especially during storm events. Ground truth of an area is necessary to calibrate the remotely sensing LIDAR and Argus systems, as well as any littoral circulation models. This requires periodic personnel-intensive bathymetric and shoreline surveys. Bathymetries and beach contours were obtained using three surveying methods: ATV, personal watercraft (PWC), and walking. An ATV rigged with an Ashtec real-time kinematic-differential global positioning system (KGPS) receiver surveyed a cross-shore distance extending from the maximum run-up at low tide to the dune face, and an alongshore area of O(1km) at each beach survey. To ensure accuracy in the ATV's position and elevation, the Ashtec KGPS was synchronized with the local base station at Sand City (List and Farris 1999). The KGPS system error when mounted on the ATV is assumed to be that of a stationary system: 1cm in the horizontal and 2cm in the vertical. The same KGPS receiver was also mounted on a backpack worn by a surveyor in the low tide surfzone to a depth of 1m and an elevation slightly higher than the closest ATV track to the shore. No error testing has been conducted yet for the walking survey, but the error is estimated to be around 10cm in the vertical and horizontal, with variations depending on the individual walker (MacMahan Personal Communication 2003). At high tide of the same day as the other surveys, a PWC equipped with a KGPS receiver and echosounder covered the area from several hundred meters offshore to about 1m of depth. When mounted on the PWC, the KGPS error is 6cm in both the horizontal and the vertical. The PWC echosounder has a horizontal spatial resolution of 0.8m and an accuracy of 3cm (MacMahan 2001). In this manner, each of the surveys overlapped the others.

Surveys were conducted over the course of the winter season, November to February, which represents the most energetic conditions in the Bay, as well as the most interesting beach morphology. Conducted at around three week intervals during the

study, Del Monte, Sand City, and Marina beaches were all surveyed within days of each other to make temporal comparisons possible.

A survey was conducted 16 January 2003 during a time of no wind and a moderate swell of $H_s = 1.7m$. Low wind and wave energy conditions are ideal to conduct the beach surveys. Too large of a significant wave height hinders the PWC's intrusion into the breaking zone and the walker's cross-shore wading distance. The survey of Del Monte Beach shows a low-tide terrace with no rip cells (Figure 5). The survey tracks of the ATV, walker, and PWC are traced in the figure, demonstrating the overlap between techniques.

The survey of Sand City Beach on the same day (Figure 6) shows a low tide terrace incised by rip channels with spacing of O(150m), similar to results during the RIPEX experiment at this same beach (MacMahan 2003a). The GPS tracks indicate that full coverage of the survey area was not achieved. The lower-most shoal in Figure 6 is generated by the Delaunay triangulation that drives MATLAB's gridding function (Barber *et al.* 1993), but the lack of sampling in that region causes those contours to be suspect. It is perhaps easier to distinguish the bathymetric features with the contour image (Figure 7); however, the cuspate features of the beach are more easily discernible in the colored plots (Figure 6). The cusps are of the same order (150m) and occur concomitantly with the rip channels. This supports the findings of Bowen and Inman (1969), Komar and McDougal (1988), Revell *et al.* (2002), and Sallenger *et al.* (2002) that the rip current channels occur in the embayments of cuspidal shorelines.

The Marina State Beach was surveyed on 16 January 2003 (Figure 8) and shows a well-resolved shoal at $y = -100m$ and a cuspidal shoreline. Qualitatively, the cuspidal spacing is O(350m) with the embayments at the mouths of the rip channels. The beach and inter-tidal area was well sampled to a depth of 1m, but the sparse PWC echosounder data makes the analysis of the rip spacing uncertain. Thus, the rip channel spacing is determined from the location of the rip channels.

Initial surveys suggest that to ensure full coverage of the beach, it would be beneficial to the surveyors if visual markers were erected. Often the PWC, ATV, and

walker did not cover the same alongshore areas; this led to gross interpolations by the Delauney bi-linear triangulation method at the upper and lower alongshore bounds (Figure 7). The surveys suggest that a hatched diagonal pattern might be adopted by the PWC and a few alongshore transects be added to the walker's survey. This would better resolve some of the embayments and beach cusps, as well as avoid many artifacts in the estimated topography. Also, unless the longshore bar is being sampled, the surfzone features of interest generally have alongshore variations, which are difficult to resolve with shore normal PWC transects. For example, offshore transverse bars at Duck, NC were not observed until captured by time-exposed video imagery because previous surveys of cross-shore transects had poor alongshore resolution (Konicki and Holman 2000).

B. LIDAR

As mentioned in the introduction, it was qualitatively found that a rip current is concomitant with each cusp embayment for the Southern Monterey Bay (Figure 4). Given this relationship, we consider cusp spacing, λ_c, to be a proxy for rip spacing, λ_{rip}. Beach surveys are used here to determine cusp spacing.

Light Detection and Ranging (LIDAR) surveys were conducted before and after the 1997-1998 El Nino winter to measure erosion along the southern coast of the Monterey Bay (Thornton et al. 2003). Determining beach cusp dimensions along the southern coast of the Monterey Bay is a byproduct of that 1997-98 study. The LIDAR imaging was part of a larger effort by the United States Geological Survey (USGS), NASA, and NOAA to map the erosional response of the western coast of the United States during that El Nino (Sallenger et al. 2002). The LIDAR survey was conducted using NASA's Airborne Thematic Mapper (ATM) mounted underneath a plane (Figure 9) and calibrated for 3-D positional accuracy as described in Brock et al. (2002). The ATM has a swath width of 350m given an aircraft altitude of 700m, a horizontal point resolution of 1.4m (Brock *et al.* 2002), and a vertical RMS error of less than 15cm (Sallenger et al. 2003).

Post-processed LIDAR images generated by the NASA's LaserMap program are loaded as geotiff files into the ArcView Geographic Information System (GIS) suite (Brock *et al*. 2002). Images are overlain on Digital Orthophoto Quadrangles with a final output displayed in UTM coordinates with NAD-83 as the horizontal datum (Figure 10). The underlying images were taken 21 August 1998, after the LIDAR survey. A shoreline is defined by MLLW, with watered areas excluded from the output by use of an edit mask. Though over-sampling the data, a grid spacing of 1 m was chosen to represent the variable ATM sampling rate (Thornton *et al.* 2003). It was deemed desirable to resolve beach cusps O(30m) in the analyses, which are difficult to resolve both near the waterline (0 m contour) and near the toe of the dune (5m contour). Therefore, the two-meter contour was chosen to represent the shoreline.

The 2m contour, plotted in UTM coordinates, was rotated 60° to provide a monotonic X-coordinate. A 2^{nd}-order polynomial was fitted, in a least square sense, to the data set and subtracted to remove the curvature of the Southern Monterey Bay (Figure 11). Some distortion is present in the vicinity of Del Monte Beach and the Salinas River, identifiable by the positive trend in y-axis deviation from zero, moving left and right from the center of the x-axis, respectively. The resulting error in shoreline length is less than 1.5 percent in these regions. To remove the distortion, the data were then high-pass filtered, removing variations greater than 1000m scale. The resulting shoreline contains cuspate features oscillating about a straight shore (Figure 12; Figure 13). Qualitatively, the spacing of the cusp features increases in length and in width from south to north after the El Nino winter.

Wavenumber spectra (m^{-1}) were generated for both surveys (Figure 14; Figure 15) to examine the lengths of the cuspate features. The spectra are truncated for wavenumbers greater than 0.05 (m^{-1}) as energy at these wavenumbers are features too small to be cuspate. The spectra were calculated by subdividing the full record into 1200m lengths resulting in twenty-two degrees of freedom for both the 1997 and 1998 surveys. The signals from both years indicate a broad peak with a peak corresponding to a 340m cusp width. The energy spectra show that for both years the dominant oscillations are similar to the spacing of rip currents. The broad spectral peak about the

value of $K_y = 0.0029m^{-1}$ ($\lambda_{cusp} \approx 340m$) is due to spectral smearing owning to the significant variability in cusp spacing. Beach cusps are evident in the 1998 LIDAR study as indicated by the broad spectral bump centered on wavenumber $0.021m^{-1}$ ($\lambda_{cusp} \approx 40m$).

To resolve the variable cusp spacing alongshore, the data were segmented into multiple bins approximately 1200m in length. Each segment contains complete cusp wavelengths to reduce leakage in the spectral analysis. Segmentation decreases the degrees of freedom available from the length of record, but the 1200m record length was chosen to measure variability and give a reasonable cusp statistic (5-10 cusps per segment).

The average cusp spacing for each bin, $\overline{\lambda_c}$, was calculated as the peak K_y of the wavenumber spectrum (Figure 16). Prior to the winter, the cusp spacing initially increases and then is more or less constant. After the El Nino winter, there is an increase in cusp lengths proceeding north toward the Salinas River. The increase in cusp spacing moving up the coast, and hence the increase in rip spacing, is consistent with both our observations and hypothesis.

The average horizontal cusp excursion,

$$\overline{\eta_c} = \sqrt{\sum_i \left(H_i^2\right)} \qquad (2.1.1)$$

where H is the horizontal excursion measured from the center of the embayment to a point parallel to the horn for each segment (Figure 17). Two trends are noticeable from a comparison of the cusp excursions of the two surveys. First, the excursions grow in size for both years as one proceeds from Monterey northward along the beach toward a more energetic wave climate. Second, the cusp excursions are noticeably greater in magnitude for the 1998 survey.

A steepness parameter is calculated as a measure of the horizontal excursion of the cusp over the alongshore cusp length:

$$m_c = \eta_c / \lambda_y \qquad (2.1.2)$$

The steepness is fairly constant for fall 1997, until alongshore distance 6000m, whereas the spring 1998 survey has much greater cusp steepness values along the entire length of the surveyed shoreline (Figure 18). This probably reflects the increase in $\overline{\eta_c}$ due to the scour and increased erosion deepening the cusp embayments during the El Nino storms.

Another LIDAR survey by the United States Geological Survey is planned for the Monterey Bay during the summer of 2003. However, the survey will only provide a snapshot of the rip spacing in the Bay. Besides cost and time constraints, LIDAR does not provide insight into the temporal variability of morphology. A need exists for auto-archived and ongoing remotely sensed time-series of nearshore processes. The Argus camera system fills that gap.

C. ARGUS

The Argus video imaging system is a means to obtain long term and beach information without the cost of traditional in-situ instrumentation. The Argus system does not survey to the same accuracy as conventional techniques, e.g. KGPS walking transects, but it is attractive for its cost, immunity to weathering, and temporal sampling ability (Stockdon and Holman 2000).

So far, only video images at Marina State Beach are processed on a regular basis. The Marina Argus station is an array of five video cameras mounted approximately 15m above the shoreline. This area of coverage is greater in the alongshore than that of the GPS surveys to date at Marina. The Sony 640x480 pixel cameras have an image resolution dependent on the distance to the object of interest, but typically are of the same order as GPS survey resolutions (1997). They are housed within standard, environmentally resistant surveillance camera housings. The protective glass window has a tendency to fog up or get dirty at this location due to its proximity to the beach and its location at the edge of the dune. The Marina cameras were initially lined up in late October, but were vandalized by bending them out of position and smearing them with surf-wax between 02NOV02 and 06NOV02, 1900GMT. They were rectified and working properly until 09FEB03, 1900GMT, at which point they were again vandalized

and knocked out of alignment. They were realigned on 20 February 2003. The five cameras are angled to cover more than 180 degrees of nearshore area with minimal overlap, resulting in a collective Field of View of 2 km alongshore and 1/2 km across shore.

Each camera generates a snapshot of the beach on the hour on a daily cycle, resulting in images from after dark being stored in the database as well. Also, a ten-minute time exposure (timex) is created each hour to show the general trends of the surf at that time. This exposure length was found to be ideal for Atlantic wave conditions and has been adopted in the Monterey Bay (Holman and Lippmann 1987). Finally, highly dynamic areas of the surf zone are shown in a variance image derived from the timex. 43200 stored images are generated over the course of the year. Needless to say, one must be highly selective of which images will be analyzed, or even viewed. Many may be culled based on the times listed, *e.g.* those at night, but others must be loaded and then visually checked for unsuitably due to foggy/low visibility conditions, salt or grime on the lens, sun-induced glare, misalignment of the camera, etc.

Ground Control Points (GCPs) are required to solve the equations needed to rectify an Argus image so that an object is known absolutely in both image and world coordinates (Holland *et al.* 1997). Preferably, GCPs of opportunity are used to save on cost and time. They might include a pier piling, tall building, fence post, or any other object that will remain in a relatively fixed location during the course of the experiment. The Marina site has a fence immediately in front of the cameras that provides several GCPs; however, its close proximity to the array means that the accuracy of its location must be great, or severe distortion will occur at the far edges of the camera's viewing field. There are a few other GPC's, including the horizon, that can be used in each of the five images generated by the array. Despite these natural validation points, a few manufactured GCPs are brought in during rectification to ensure the process is accurate and points are scattered throughout the images. Self-employed GCPs are typically large white spheres that are placed in the cameras' viewing window, have their GPS coordinates recorded, and are identified in a grayscale image by their large contrast with the beach and ocean (Holland *et al.* 1997). Rectification allows the scene captured by a

camera's lens to be transformed from image coordinates (U and V) into more familiar world coordinates (X and Y) (Konicki and Holman 2000). It standardizes the different views presented by each camera in the array, and allows their collective image intensity maps to be smoothly merged into one plan view of the beach (Figure 19). For a three camera system at elevation 10m and near to the survey area, Holland *et al.* (1997) obtained world coordinate errors of O(1m) for the rectified images. This order is the same as the error by traditional surveys (Salinger 2003) and is extended to the five camera Argus system at Marina.

Previous experiments have successfully compared traditional in situ morphological surveys with Argus timex imagery. Konicki and Holman (2000) confirmed the location of transverse sand bars at Duck, NC using both the Coastal Research Amphibious Buggy (CRAB) and an Argus array. However, accurately identifying individual rip occurrences from these images is still a nascent technique.

Ranasinghe *et al.* (1999) used zero upcross/downcross analysis to locate rips at Palm Beach, Australia. Those rips were easily distinguishable by visual observation at the shoreline as dark patches of water with little foam or wave breaking, and consequently as troughs in the longshore transects of pixel intensity generated from the Argus time exposures. This technique is not adequate for Marina State Beach, as the rips tend to be obscured by resident foam and surfactants on the water's surface and therefore present smaller longshore pixel intensity gradients in the images (Symonds Personal Communication 2003). Also, the Marina camera is only 15m above the survey area, while the Palm Argus setup commands a view from approximately 100m up on a bluff overlooking the survey area. A view from a higher incidence angle would allow for a greater field of view and capture more rips in the time exposures.

Another method employed by nearshore researchers is to study the lagged autocorrelations function (ACF) of the alongshore intensity transects. Quantitatively, the lag of the local maximum of the correlation coefficient is noted as the rip spacing for that imaged area (Ranasinghe *et al.* 1999). Peaks in that function at a 95% confidence interval were looked for by Ranasinghe *et al.* (1999) in their Palm Beach, Australia analysis. Unfortunately, the rips lacked periodicity in their spacing and the ACF

generated no statistically significant peaks. Given the gradient in rip spacing demonstrated by the morphology and LIDAR surveys, we would be ill advised to use this method in the Monterey Bay.

Though not as rigorous, this study estimates λ_{rip} from visual analysis of a large sample of timex images at Marina during the months of the GPS beach morphology surveys. Preferential wave breaking over a shoal is represented by a large pixel gradient in that area of the timex image. Gradients in bathymetry are inferred from these pixel gradients. Rip currents are clearly visible in the rectified Argus images of Marina Beach as areas of low intensity pixels extending seaward with surrounding high intensity pixels of shoal-breaking waves. Close attention was paid to 16 January 2003 and 14 February 2003, dates when all three beach survey methods worked in unison. Unfortunately, the cameras were jarred out of alignment just prior to 14 February 2003 and were not geometrically realigned by that time. Consequently, images from 8 February 2003 and 14 February 2003 were used as proxies, with consequent reservations about temporal and spatial applicability (MacMahan 2003a) for the actual survey date. Average λ_{rip} spacing during the study was of O(300m) at Marina Beach. The method employed to measure rip spacing via video imagery at Marina is accomplished by hand analysis of images generated once weekly from November 2002 to April 2003. This qualitative assessment of rip spacing over the energetic winter season gives λ_{rip} estimates of O(300m). This is in agreement with our morphological surveys of the area (Figure 8), as well as the energy-K_y plots of that bin from the LIDAR survey (Figures 14 and 15).

Contoured images from the beach surveys are overlaid on their respective Argus images (Figure 20). Qualitatively, a strong correlation is present between the breaker-line in the Argus image (represented by the line of white pixels just offshore), and the narrowing of the contours in the GPS survey images (rhythmic longshore bars). The cusps identified by the walking survey at Marina on 16JAN2003 are almost perfectly overlaid with the white pixel undulations between 50-100m across shore. The rhythmic pixel pattern in the Argus image repeats at O(350m). Ground truthing of the shore normal alternating streaks of white and dark pixels as rip channels and connected bars is

difficult given the incomplete coverage of the PWC survey during any of the Marina surveys. Though not concurrent, the Argus timex of 08FEB2003 and the PWC transect of 14FEB2003 both indicate the presence of a strong rip current at approximately $x = 0m$ alongshore (Figure 20; Figure 8). Unfortunately, the PWC surveys only covered 20% of the Argus field of view, thereby preventing any other features from being validated. No walking or ATV survey was archived for that date, so a verification of Argus–imaged beach cusps is not available.

III. WAVE CLIMATE

A. WAVE ENERGY AND DIRECTION

To test the hypothesis that the rip current spacing is a function of wave energy and or wave directional spread, directional wave parameters are compared between measurements obtained from two Datawell Directional-Waverider buoys at Marina State Beach and Sand City Beach, both in 18m of depth (Figure 21). These two sites are separated by ~6km. To compare the variation in wave parameters along the shoreline of the Southern Monterey Bay, a time period of yeardays 120 to 188, 2002 was chosen for analysis when both waverider buoys were operating. These measurements are used to test both a refraction and nearshore circulation model.

The energy of an incoming wave train is described by the directional spectrum:

$$S(f,\theta) = S(f)D(f,\theta) \tag{3.1.1}$$

where θ signifies the arbitrary incidence angle of a wave train. The directional spectrum can be represented as a Fourier series in direction at a particular frequency:

$$\begin{aligned} D(f,\theta) &= \frac{1}{\pi}\left[\frac{1}{2} + \sum_{n=1}^{2}\{a_n\cos(n\theta) + b_n\sin(n\theta)\}\right] \\ &= \frac{a_0}{2} + a_1\cos\theta + b_1\sin\theta + a_2\cos 2\theta + b_2\sin 2\theta \end{aligned} \tag{3.1.2}$$

Longuet-Higgins *et al.* (1963) demonstrated that the first four Fourier coefficients could be derived from the spectra and cross-spectra of the pitch, roll, and heave of a buoy or equivalently, the pressure and horizontal velocity components (p,u,v).

$$\begin{aligned} a_1(f) &= \int_{-\pi}^{\pi} d\theta\cos\theta S(\theta;f) \\ &= \frac{C_{pu}(f)}{\{C_{pp}(f)[C_{uu}(f) + C_{vv}(f)]\}^{1/2}} \end{aligned} \tag{3.1.3}$$

$$b_1(f) = \int_{-\pi}^{\pi} d\theta \sin\theta S(\theta; f) = \frac{C_{pv}(f)}{\{C_{pp}(f)[C_{uu}(f) + C_{vv}(f)]\}^{1/2}} \quad (3.1.4)$$

$$a_2(f) = \int_{-\pi}^{\pi} d\theta \cos 2\theta S(\theta; f) = \frac{C_{uu}(f) - C_{vv}(f)}{C_{uu}(f) + C_{vv}(f)} \quad (3.1.5)$$

$$b_2(f) = \int_{-\pi}^{\pi} d\theta \sin\theta S(\theta; f) = \frac{2C_{uv}(f)}{C_{uu}(f) + C_{vv}(f)} \quad (3.1.6)$$

Both the buoy and ADCP data are archived with energy and these low-order coefficients at each frequency bin.

The waves at the two sites are compared using parameters for height, direction, and energy flux. Significant wave height is calculated:

$$H_s = 4 * \sqrt{\int_{0.04\,Hz}^{0.25\,Hz} S(f) df} \quad (3.1.7)$$

where the frequency integral is taken across the wind-swell energy band (0.04-0.25 Hz). H_s is similar at the two beaches for this springtime series, with Marina having slightly higher waves on average ($H_s = 1.3m$) compared to Sand City, $H_s = 1.1m$ (Figure 22). The exceptions are at yeardays 142 and 152. In those instances, the significant wave height is much greater at Marina. Yearday 160 shows an event in which the wave energy is greater at Sand City. This seems to be an anomaly for this time series and is not repeated elsewhere.

The peak period, T_{peak}, is calculated from the energy spectra as the inverse of the frequency containing the maximum amount of energy:

$$T_{peak} = 1 / f_{peak} \quad (3.1.8)$$

The peak periods T_{peak}, as are expected, do not show much variation between the two locations (Figure 23).

The mean direction of the peak energy is defined in terms of (3.1.3) and (3.1.4):

$$\overline{\theta}_{peak} = \tan^{-1}\left(\frac{b_{1(f_{peak})}}{a_{1(f_{peak})}}\right) \qquad (3.1.9)$$

where the peak represents the frequency of maximum incident energy at the sensor, which is valid only if $S(f)$ is narrow-banded (Herbers *et al.* 1999), as is most common in the Monterey Bay (MacMahan *et al.* 2003). Refraction within the bay tends to result in waves approaching the shoreline shore-normal. Marina has $\overline{\theta}_{peak} \cong 7^{\circ}$ and Sand City $\overline{\theta}_{peak} \cong 2.5^{\circ}$, indicating that the wave climate at Marina is not as strongly refracted as that at Sand City (Figure 24).

Peak and bulk directional spreading parameters are calculated from the directional coefficients:

$$\sigma_{peak} = [2(1 - a_{1\_peak}^2 + b_{1\_peak}^2)^{1/2}]^{1/2} \qquad (3.1.10)$$

$$\sigma_{bulk} = [2(1 - a_{1\_bulk}^2 + b_{1\_bulk}^2)^{1/2}]^{1/2} \qquad (3.1.11)$$

which are also strictly valid only for narrow-banded $S(f,\theta)$. The spreading coefficients represent the half-width location of $S(\theta, f)$ when plotted against $\overline{\theta}_{peak}$ and $\overline{\theta}_{bulk}$, and indicate the distribution of energy about the mean direction (Figure 25).

The measured peak directional spreading parameter (3.1.10) was the same for both Sand City and Marina, $\sigma_{peak} = 14^{\circ}$. The bulk directional spreading parameter was slightly larger at Marina, $\sigma_{bulk} = 20^{\circ}$, compared with $\sigma_{bulk} = 18^{\circ}$ at Sand City. The larger σ_{bulk} at Marina suggests greater directional bandwidth at higher frequencies, as this site is more open to waves and wind from offshore.

Alongshore sediment transport is a function of the alongshore energy flux, F_y. Hence, energy flux is used to parameterize morphology, which is a manifestation of

gradients in sediment transport. Both along- and cross-shore energy fluxes are calculated. The measured energy flux is obtained from the directional spectrum:

$$F_x = \rho g \int_{f_1}^{f_2} dfc_g(f) \int_{-\pi}^{\pi} d\theta \cos\theta S(f,\theta) \qquad (3.1.12)$$

where ρ is the density of seawater, g is the acceleration of gravity, f_1 and f_2 represent the wave frequencies to be integrated across, and c_g is the group velocity. Using(3.1.3) and (3.1.4), the cross-shore bulk energy flux is:

$$F_{x\_bulk} = \rho g \int_{0.04Hz}^{0.25Hz} dfc_g(f) a_1 \qquad (3.1.13)$$

and the alongshore bulk energy flux is:

$$F_{y\_bulk} = \rho g \int_{0.04Hz}^{0.25Hz} dfc_g(f) b_1 \qquad (3.1.14)$$

The signs of both the flux parameters indicate the direction of bulk transport of the wave energy at each site. Negative F_{x_bulk} values indicate onshore transport, while positive F_{y_bulk} values represent an energy flux directed northwards toward the Salinas River.

Both Sand City and Marina (Figure 26) exhibit strong onshore transport of energy. There is a noticeable gradient between the two sites with Marina having an average cross-shore flux of $\overline{F}_x \cong 33000(J/m^2)$ and Sand City $\overline{F}_x \cong 28000(J/m^2)$. This gradient is not surprising given the significant wave height differences between the two sites.

There is significantly more variation in the direction of the longshore energy fluxes for both Sand City and Marina (Figure 27). Marina measured $\overline{F}_y \cong 3250(J/m^2)$, while Sand City measured $\overline{F}_y \cong 440(J/m^2)$. These values are a result of the increased incidence angle at Marina compared with Sand City.

B. COMPARISON WITH REFRACTION MODEL

Directional wave spectra are calculated by refracting the directional wave spectra measured at NOAA buoy 46042 (Figure 28) located in deep water outside Monterey Bay (O'Reilly and Guza, 1998). From the refracted directional spectra, time series of H_s and $\overline{\theta}_{peak}$ are generated for locations corresponding to the two Datawell buoys. The model bulk energy is calculated for the same swell-wind frequency bands as the in-situ buoys use.

The measured and refracted model H_s values are compared at Sand City and Marina (Figures 29 and 30). Linear regressions of the modeled and in-situ data show the poor correlation at both of the locations (Figures 31 and 32). The refraction model underestimates the significant wave heights by about 60% at Marina and 50% at Sand City.

THIS PAGE INTENTIONALLY LEFT BLANK

IV. RIP CURRENT SPACING RELATED TO WAVE CLIMATE

A. LIDAR

No direct comparison of the LIDAR 2m contour analysis and wave climate is possible as no working directional wave buoy was deployed within the Monterey Bay during that time, and NOAA's offshore directional wave buoy just outside of the Bay was inoperable that winter. The LIDAR imagery only contains data from pre- and post-El Nino events; therefore, it might be premature to extend these findings to non-El Nino winter shoreline morphology in the Monterey Bay (Sallenger et al. 2002).

LIDAR was also applied to the analysis of the 1997-98 El Nino-induced erosion in the Netarts Littoral Cell, Oregon (Revell, Komar and Sallenger 2002). They found that greatest amount of erosion in the dunes of the Netarts Cell occurred in the rip current embayments. Extension of this finding to the Monterey Bay would support our hypothesis that the rip currents are located at the center of the embayments.

The wavelength of cusps increased to the north, so they are not spatially homogenous. Using another analysis technique, such as wavelets, instead of Fourier transforms might increase the degrees of freedom for our shortened segments and hence the accuracy of our results. That method should be considered for future research.

B. ARGUS

Argus allows the determination of morphological changes in response to waves on an hourly basis. A current proposal by the Naval Postgraduate School Oceanography Department calls for the replacement of the existing camera housings with improved versions equipped with automated windshield wipers at Marina. Additionally, cameras will be added at Sand City and the MISO site to allow for better quantification of the morphological variation along the shoreline of the Southern Monterey Bay over time. Combined with the improved GPS surveys and contouring methods (objective analysis) at the MISO site, Sand City, and Marina scheduled for this summer, a more quantitative analysis of the rip spacing from the Argus imagery will be possible.

C. WAVE CLIMATE

Hopefully, future analysis will allow wave climate and morphological data to be compared for the same time period. It is presumptuous to draw conclusive results and parameter relationships for rip spacing from wave climates of a different season. As an example, for the Marina site, climatological wave height measurements over 5.5 years in the early 1990's show an average difference of one meter in significant wave height between the energetic winter season and the more calm summer season. Our morphological beach surveys chronicled the monthly changes in bathymetry at the three sites during the winter of 2002-03, which was also an El Nino winter. The LIDAR surveys only represented snapshots of the conditions at two short intervals in October 1997 and April 1998, respectively. No details were documented during the 1997-98 El Nino winter. Wave statistics were analyzed for yeardays 122-188 of 2002 because this was when both of the Naval Postgraduate Schools directional wave-riding buoys were operational.

D. REFRACTION MODEL

Significant efforts have been undertaken to model the directional distribution of nearshore wave trains (Munk and Traylor 1947; Abreu *et al.* 1992; O'Reilly and Guza 1991,1998). Data from wave buoys is crucial for in-situ information and ground truthing of modeled data; however, many coastal areas, especially those alien to our shores but of interest to the Navy and the Marine Corps, do not have sufficient buoy coverage to allow for precise interpolation of local wave climates and nearshore circulation.

O'Reilly's pure refraction wave model was initialized and run for the same time period as the wave buoy measurements. The model under-predicted the wave heights compared with the buoy measurements by O(50%) at Sand City and Marina. Efforts are being made to improve the refraction model. The hope is that once the refraction model is verified, it can be used to predict the wave heights, energy flux, and directional bandwidth along the entire shoreline of the Southern Monterey Bay. In addition, it is hoped that the refraction model can extrapolate NOAA buoy measurements of wave

climate off the Farallon Islands (the nearest wave buoy to the north) to Monterey Bay during the time of the 1997-98 LIDAR measurements.

E. MORPHODYNAMIC MODEL

Directional spreading is a parameter that has only recently been included in nearshore circulation models. Reniers *et al.* (2003) ran calculations using the morphodynamic model Delft 3-D for various values of directional spreading with mean angle normally incident and holding wave height constant, $H_s = 1m$ (Figure 1). The absence of directional spreading, $\sigma_\theta = 0^\circ$, led to a minimum spacing of the rip currents, consistent with a self-organizing generation mechanism. A small amount of σ_θ transformed the beach into a quasi-forced system with preferred rip spacing governed by the incoming wave groups (Figure 1). Further increasing of σ_θ caused the rip spacing to decrease as the alongshore length scales of the wave groups grew smaller (Figure 33).

Given that both Marina, $\overline{\sigma}_{bulk} = 20^\circ$, and Sand City, $\overline{\sigma}_{bulk} = 17^\circ$, fall on the shallow negative slope of Reniers' model (Figure 33), there should not be a large difference in their rip spacing for the same wave heights. The nearshore model predicts a spacing of approximately O(180m) for the two sites for $H_s = 1m$. These spacings are significantly less than the actual λ_{rip} measured for Marina, $\lambda_{rip} \cong 340m$, and slightly less for Sand City, $\lambda_{rip} \cong 150m$. Reniers (Personal Communication 2003) has run the Delft 3-D model and found that the rip spacing increases with increased wave height, consistent with the observations in Southern Monterey Bay. Future use of the model should focus on varying the incident energy of the wave fields.

THIS PAGE INTENTIONALLY LEFT BLANK

V. CONCLUSIONS

Rip current spacing in the Southern Monterey Bay is compared with the alongshore gradient in wave climate to determine if a relationship existed. It is hypothesized that the energy and directional spreading of the wave trains determined the spacing of the bay's rip channels. Monthly beach morphology surveys during 2002, LIDAR surveys from the 1997-98 El Nino winter, and Argus time exposures from the winter and spring of 2002 are used to quantify the width of the rips both spatially along the coast and temporally throughout these seasons. Significant wave height and directional spreading parameters are compared using measurements obtained for directional wave-rider buoys at Sand City and Marina for yeardays 120 to 188 for 2002. The hypothesis is tested against the in-situ data, and then against the O'Reilly Refraction model and the Delft 3-D morphology model. Directional spreading does not vary substantially between Sand City and Marina for the climatology data, and therefore does not appear to be significant for determining rip current spacing in Southern Monterey Bay. Significant wave height and energy flux should be researched further to assess their relation to the rips.

The sites of Sand City and Marina State Beach along the Southern Monterey Bay coastline with $\sim 6km$ separation between them (Figure 21) allow for general conclusions regarding the gradient of wave parameters and rip current spacing along the southern coast of the Bay. Rip spacing does indeed increase along the Southern Monterey Bay towards the Salinas River. This hypothesis is validated with qualitative rip spacing measurements from beach morphology and Argus surveys, as well as quantitative LIDAR-generated measurements of the cuspate oscillations of the Southern Monterey Bay as a proxy for rip spacing. A spacing of O(150m) is found for Sand City, while the spacing for Marina is O(340m).

It is hypothesized that each cusp embayment contains a rip channel for the Southern Monterey Bay. The order scaling of the alongshore wavenumber, $K_y = 2.9x10^{-3}m^{-1}$ ($\lambda_{cusp} = 340m$), from the LIDAR 1997-1998 cusp analysis is in

agreement with the measured rip widths, $\lambda_{rip} = 340m$, for the Southern Monterey Bay as measured by beach morphology surveys and Argus imagery during winter 2002-2003. Therefore, cusp spacing is a good surrogate for rip current spacing.

Argus images are capable of remotely measuring rip current spacing over large spatial and temporal scales. Qualitative measurements of rip current spacing during winter 2002-2003 at Marina are found to be O(350m), in agreement with beach morphology surveys during the same period at that beach. They are obtained by inferring bathymetry gradients from pixel gradients in the images. Offshore features at Marina are sometimes difficult to distinguish, either due to dirty camera lenses and a low camera elevation above the beach, or to resident foam and surfactants smoothing the pixel gradient in the time exposures.

Peak Directional Spreading, $\overline{\sigma}_{peak} = 14^{\circ}$, does not vary between Sand City and Marina during the study, while bulk directional spreading has a small variation with Marina $\overline{\sigma}_{bulk} = 20^{\circ}$ and Sand City $\overline{\sigma}_{bulk} = 18^{\circ}$. Directional spreading does not appear to be the dominant factor in the rip current spacing in the Southern Monterey Bay. The gradient of both significant wave height, and cross-shore wave energy flux between Sand City and Marina should be considered in relation to the rip spacing and nearshore morphology for these locations in future studies and predictive models.

O'Reilly's wave refraction model under-predicts by O(50%) the significant wave heights calculated by the directional wave buoys at both Sand City and Marina. Therefore, O'Reilly's model could not be used to extrapolate the wave climate along the shoreline of Southern Monterey Bay.

The difficulty of this study is that the wave climate that generated the cusps and rips of varied lengths is not known. The cusps could have been generated by a single extreme storm having particular characteristics, and then persisted for a long duration. Therefore, we cannot make definitive conclusions regarding our hypothesis.

It has been demonstrated that the tools to answer the hypothesis are now in place, including the Argus system to examine temporal process changes, wave measurements,

and periodic in situ surveys for verification. In addition, frequent 2m contour surveys are being conducted by driving along the beach with a KGPS mounted on the ATV.

FIGURES

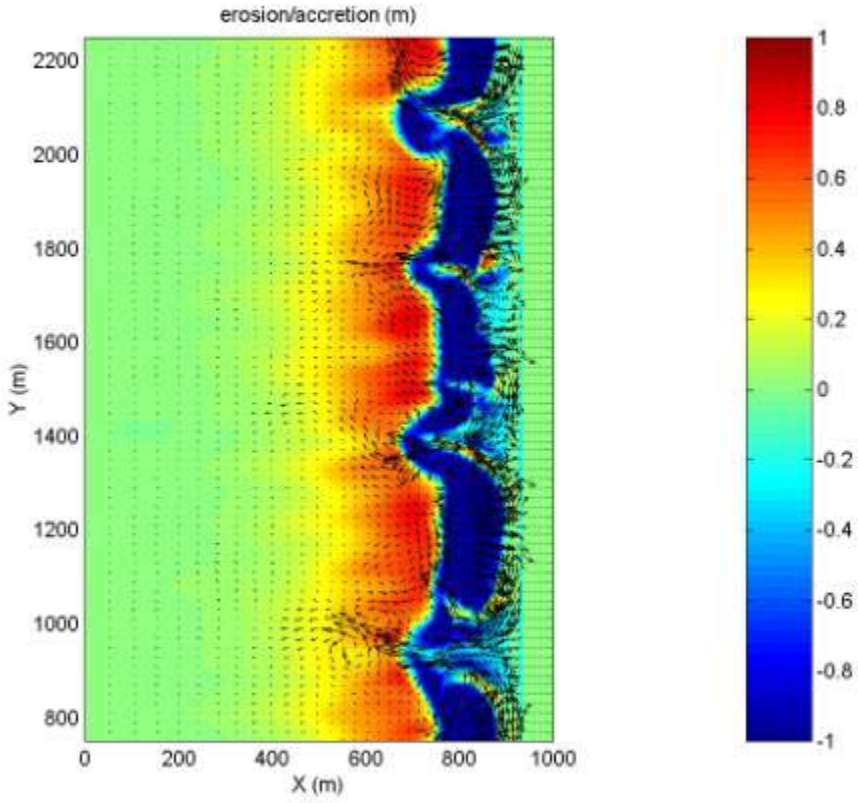

Figure 1. Example of rip currents and underlying bathymetry of a barred beach incised by rip channels generated by a research version of the Delft 3-D morphodynamic model (Reniers *et al.* 2003). Erosive areas are shown in red while areas of accretion are in blue. Waves on the outer boundary are directionally broad with $H_s = 1m$ and $\overline{\theta}_{mean} = 0^\circ$. The initial bathymetry is an alongshore uniform barred profile.

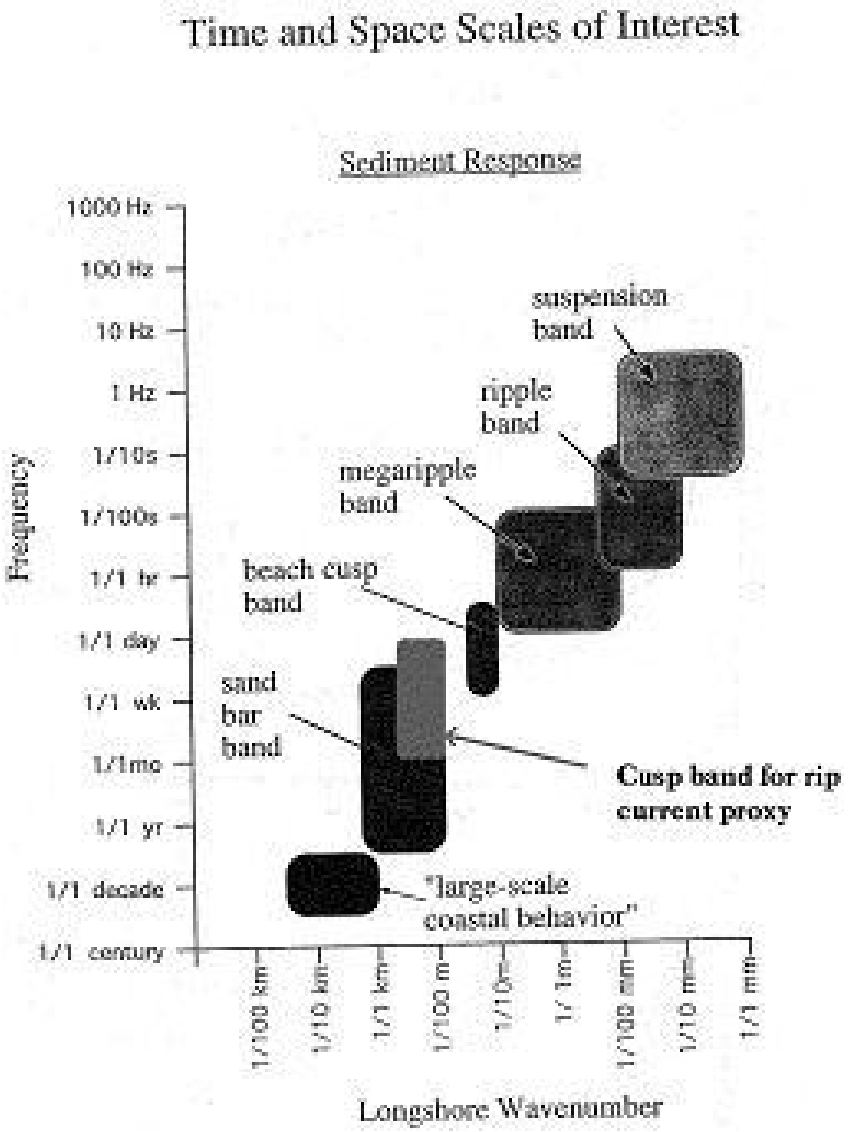

Figure 2. Shoreline and sediment organization oscillations as a function of frequency and alongshore wavenumber K_y. The cuspate features of interest vary between one day→one month temporally, and 100m→500m spatially (from Komar 1998).

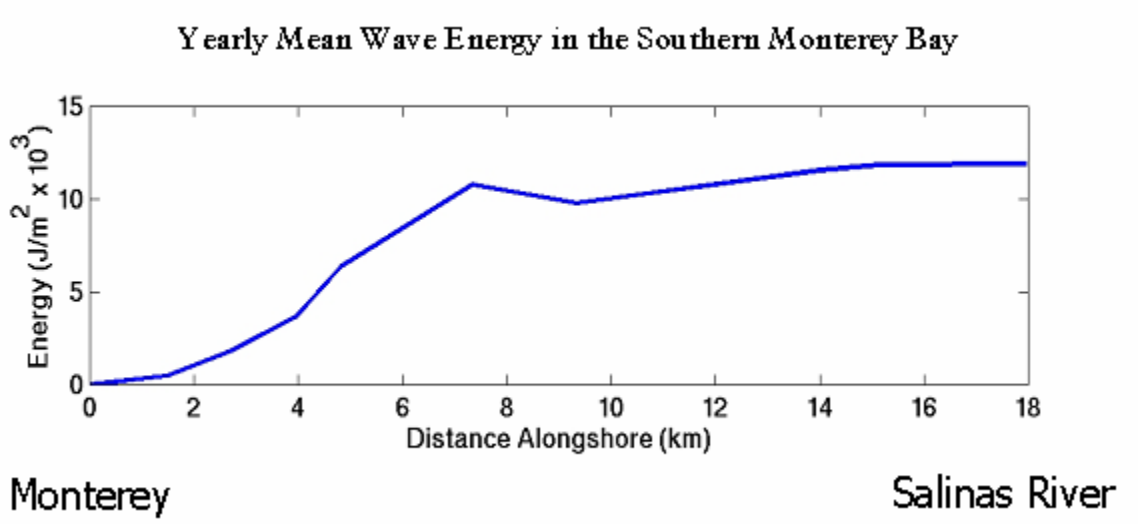

Figure 3. Mean wave energy derived from twenty years of offshore climatology refracted to the 10m contour, showing a large alongshore gradient in wave climate exists in the Southern Monterey Bay due to the shadowing effects of Point Pinos at Monterey Wharf Number 2 (0 km) and the wave focusing at the Salinas River (18km) from refraction by the Monterey Canyon in the center of the Bay.

Figure 4. Aerial photo of Southern Monterey Bay taken at low tide on April 1984 with energetic wave conditions showing large beach cusps associated with rip current cells. The cusps and rips are both of O(100-400m) (Thornton *et al.* 2003).

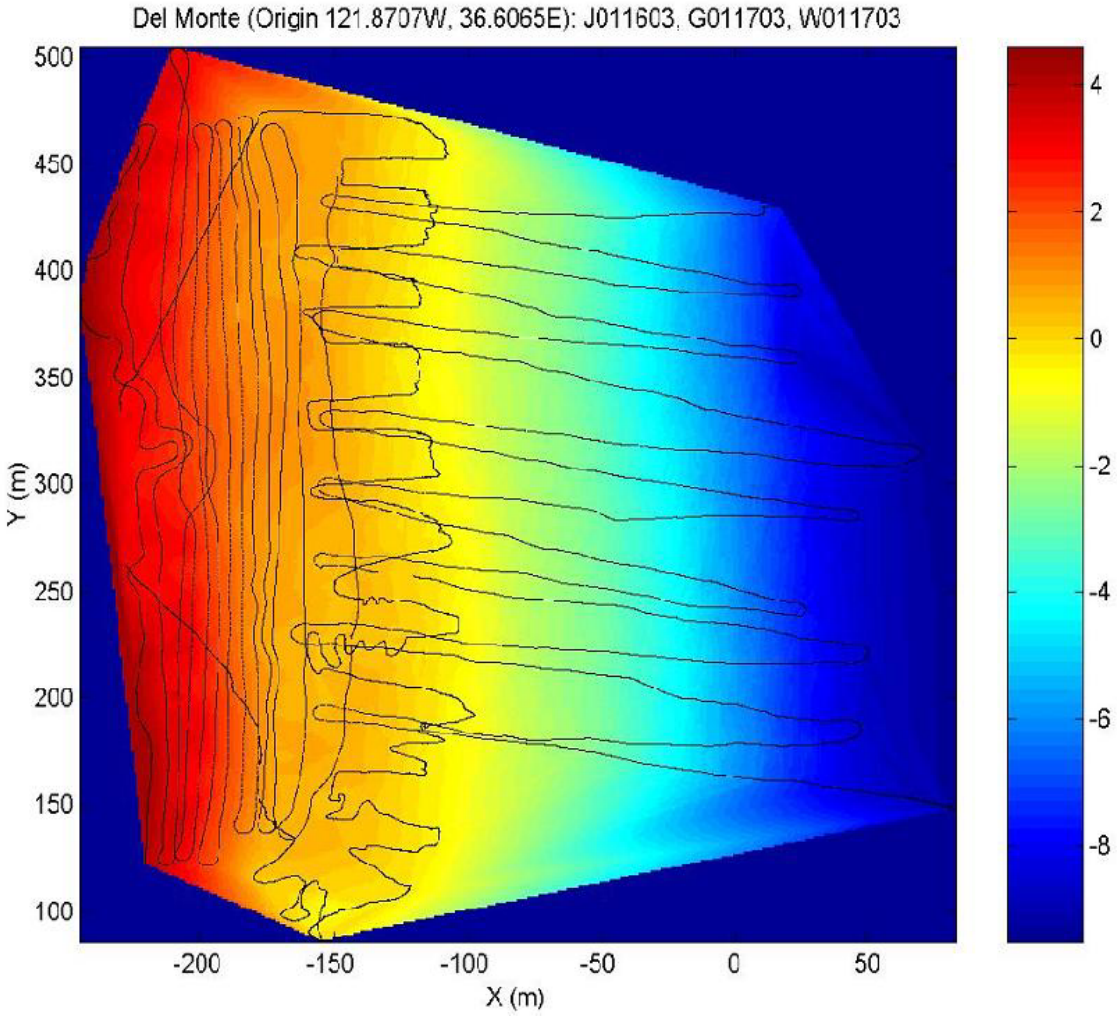

Figure 5. Morphological survey of Del Monte Beach, Monterey Bay, CA using kinematic GPS and an echosounding transducer. The black lines represent, from left to right, the tracks of the ATV, walker, and PWC. The morphology is a shallow sloped barred beach with no visible rip channels.

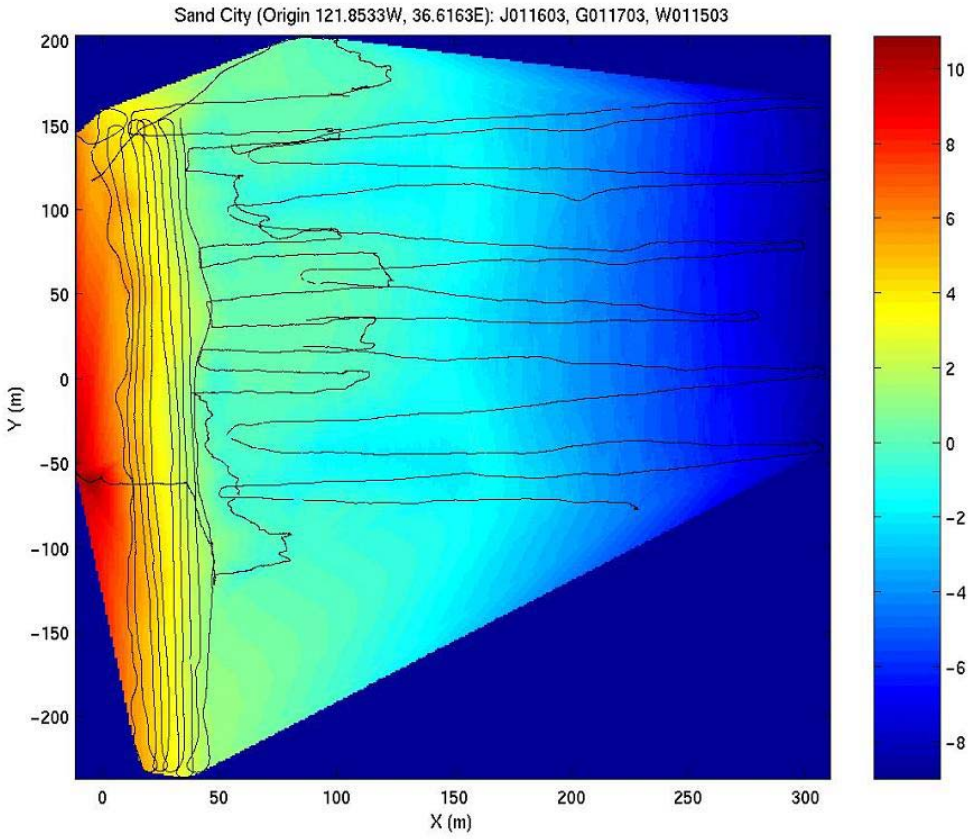

Figure 6. Morphological survey of Sand City Beach, Monterey Bay, CA using kinematic GPS and an echosound transducer. The black lines represent, from left to right, the tracks of the ATV, walker, and PWC. A system of shoals and embayments is clearly visible with spacing O(150m).

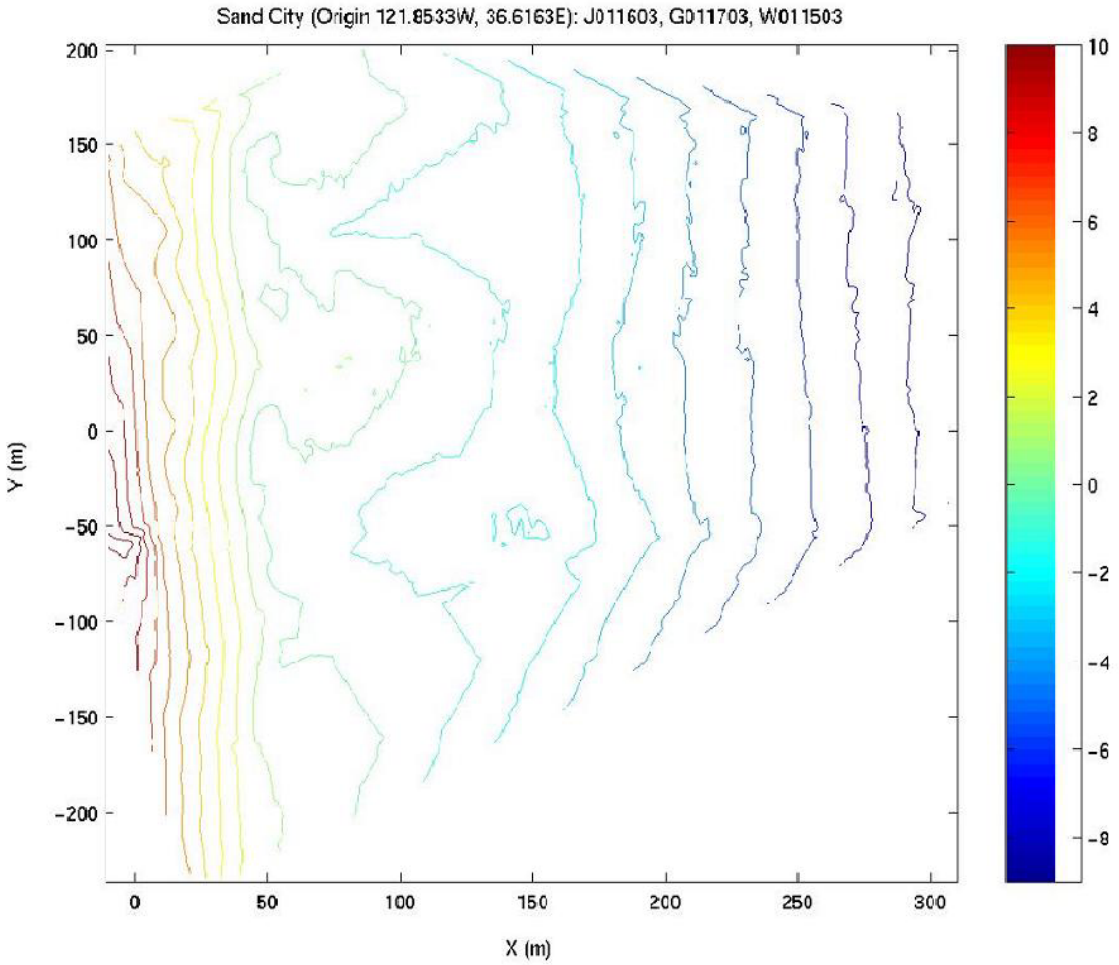

Figure 7. The survey results from 16 January 2003 at Sand City, Monterey Bay, CA using vertical contours. The rip current embayments are clearly visible at $y = -50m$ and $y = 100m$.

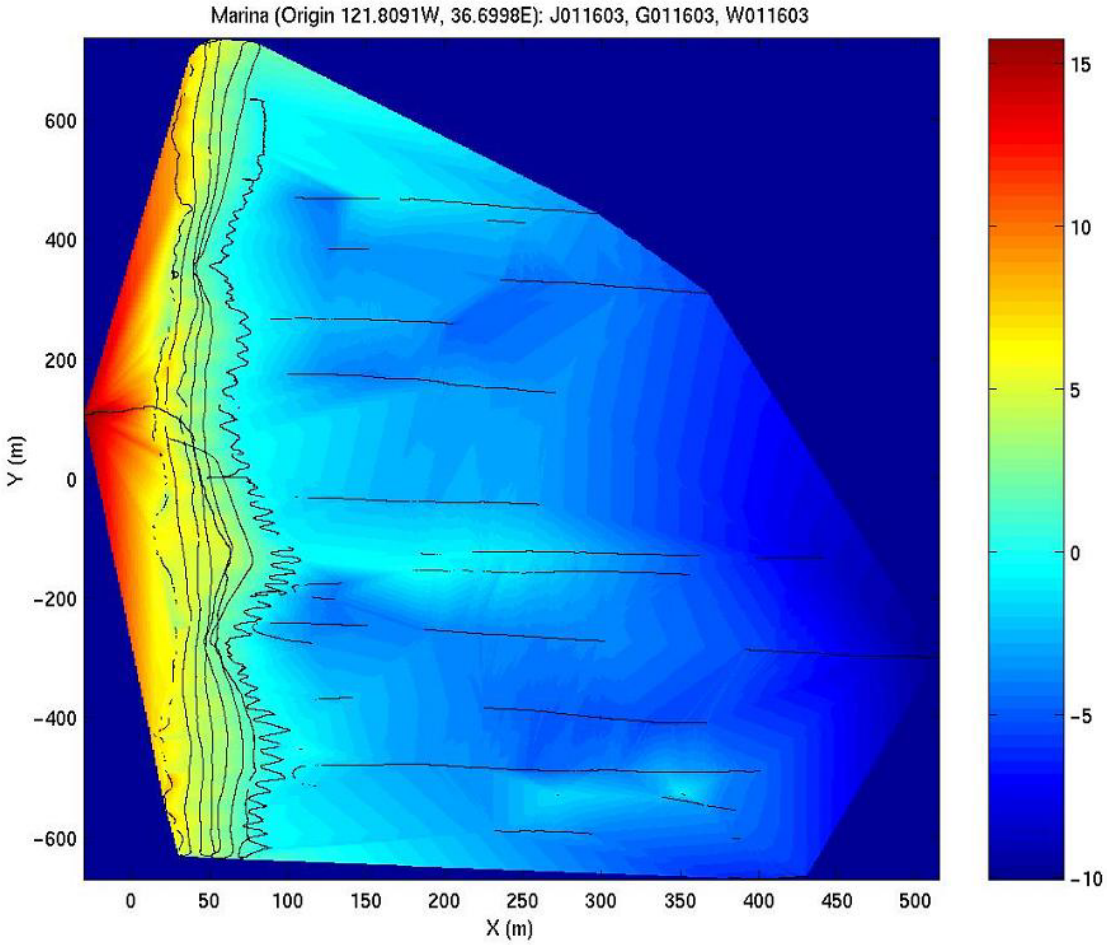

Figure 8. A cuspate shoreline with rip current circulation cells of O(300m) is evident at Marina State Beach, Monterey Bay, CA from this three-part GPS/echosounder survey on 16JAN2003. Rip currents are located O(200m) apart at Y=200m and Y=-200m.

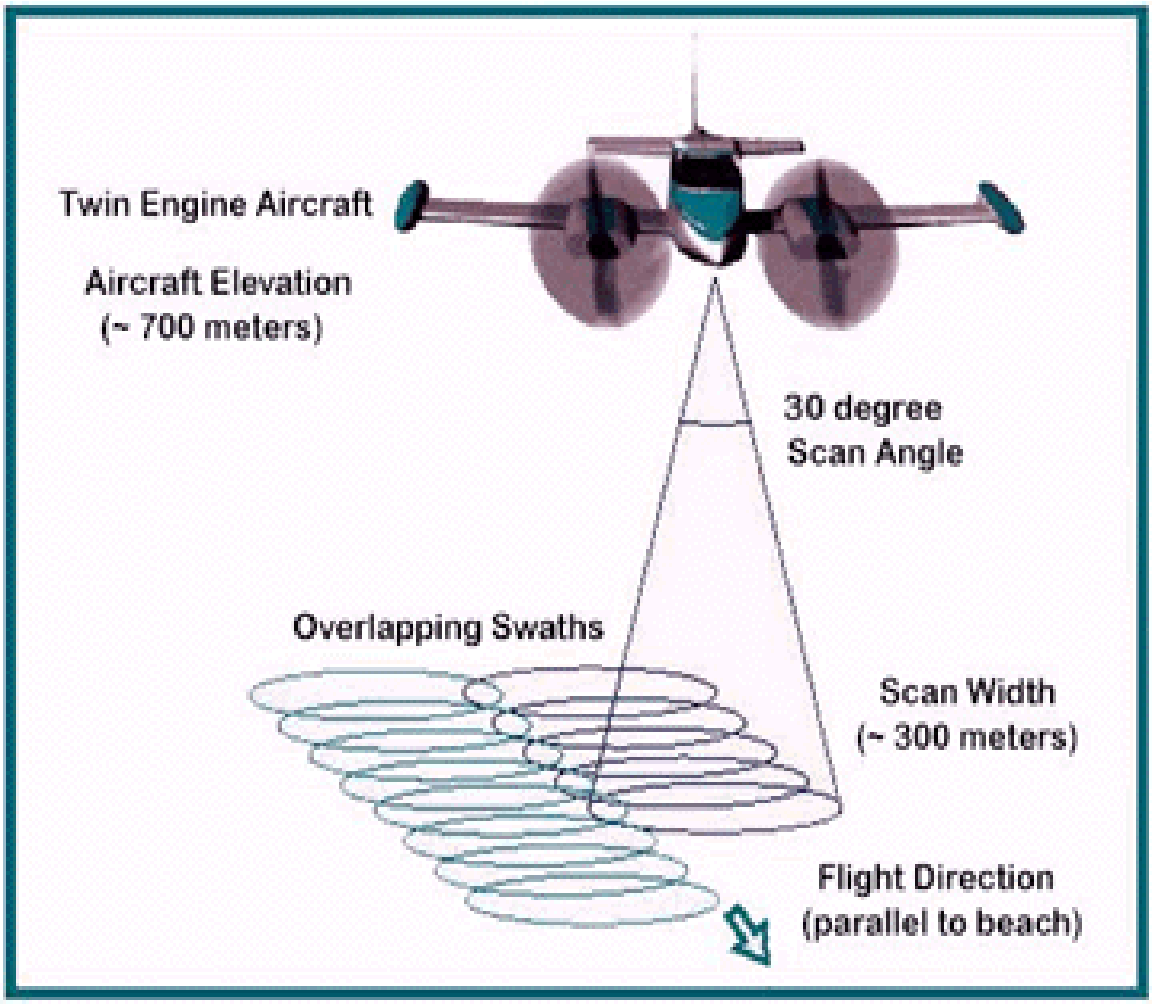

Figure 9. A typical Airborne Topographical Mapper flight: surveys conducted October 1997 and April 1998. Horizontal point resolution is O(1.4m) and vertical RMS resolution is O(15cm).

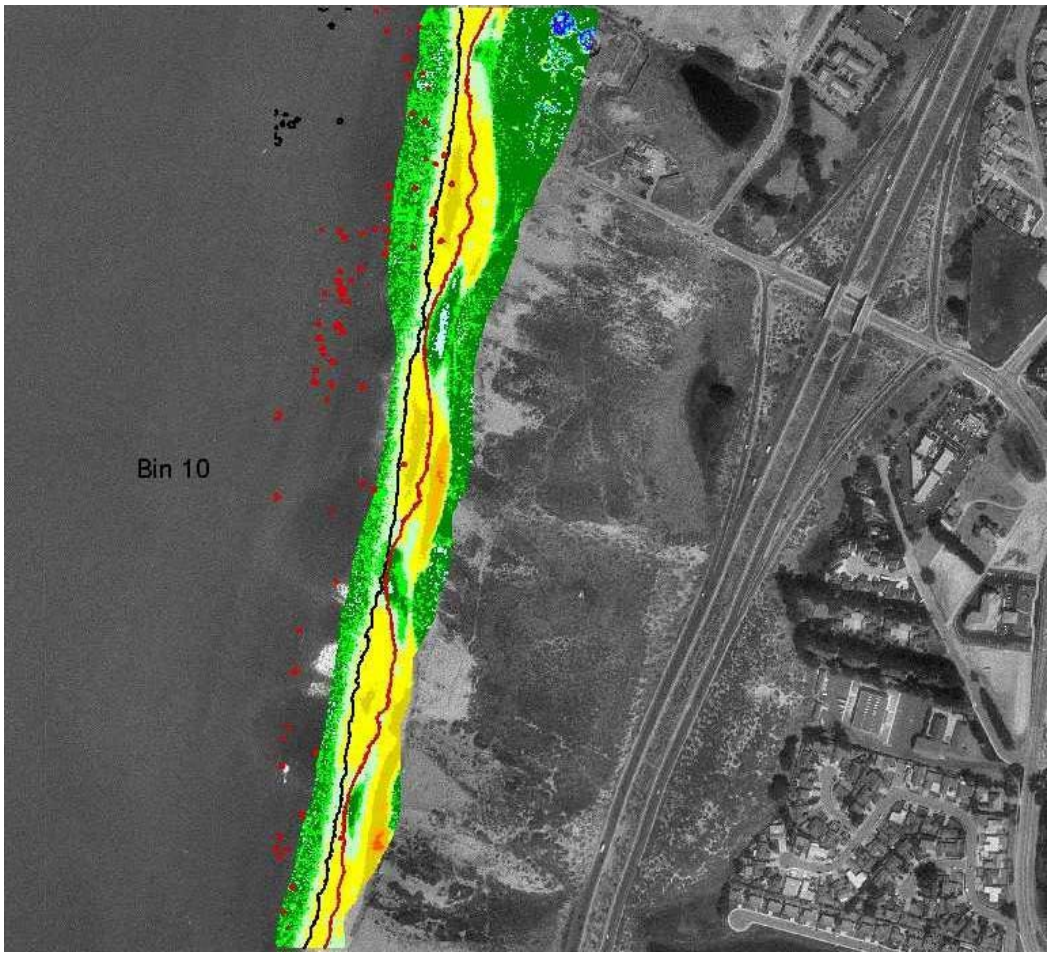

Figure 10. Example of a processed 2m contour generated by NASA's Airborne Thematic Mapper overlain on a difference survey, with both overlain on an aerial photgraph of the Southern Monterey Bay taken near the time of the 1998 LIDAR survey. The black line represents the 2m contour in 1997, with 1998 in red. This contour was chosen specifically to resolve beach cusps O(30m) and larger features.

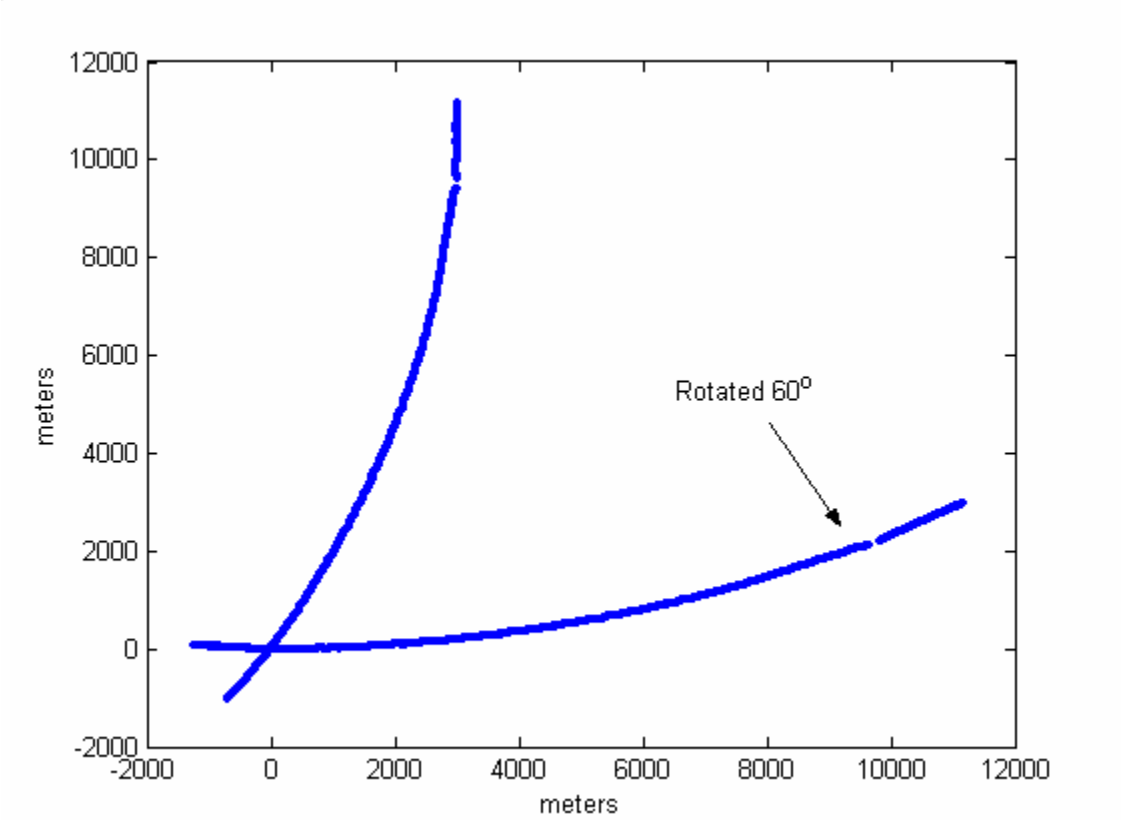

Figure 11. Raw signal of the 1997 LIDAR data, plotted in UTM coordinates. The curve was rotated 60° to insure monotonicity along the x-axis.

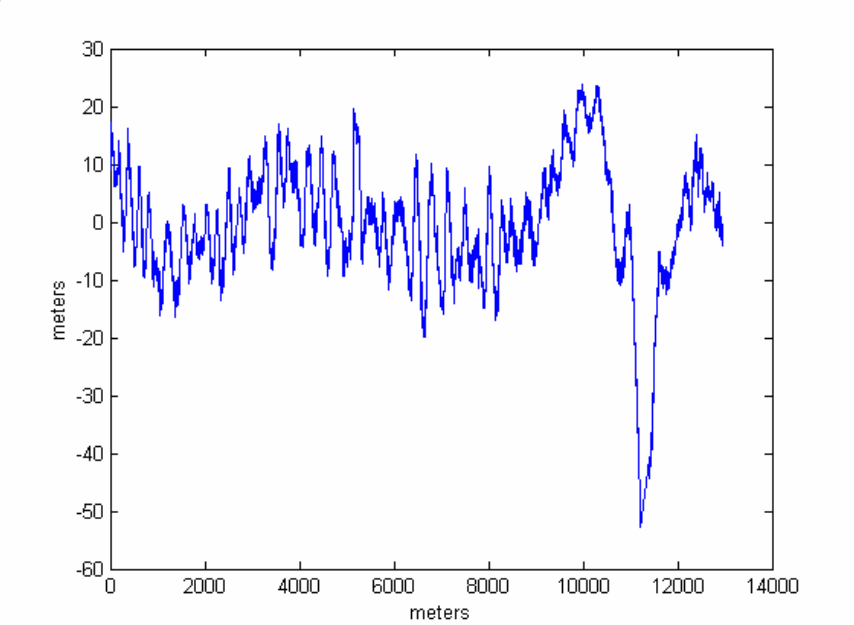

Figure 12. 2m contour for Southern Monterey Bay from the 1997 LIDAR survey, after subtracting a 2nd-order polynomial to remove the curvature of the coastline and high-pass filtering to remove oscillations greater than 1000m.

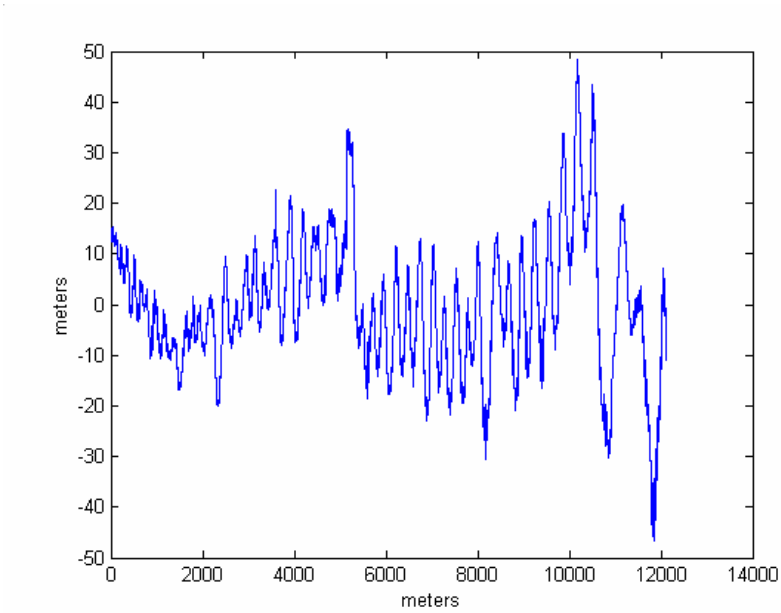

Figure 13. 2m contour for Southern Monterey Bay from the 1998 LIDAR survey, after subtracting a 2nd-order polynomial to remove the curvature of the coastline and high-pass filtering to remove oscillations greater than 1000m.

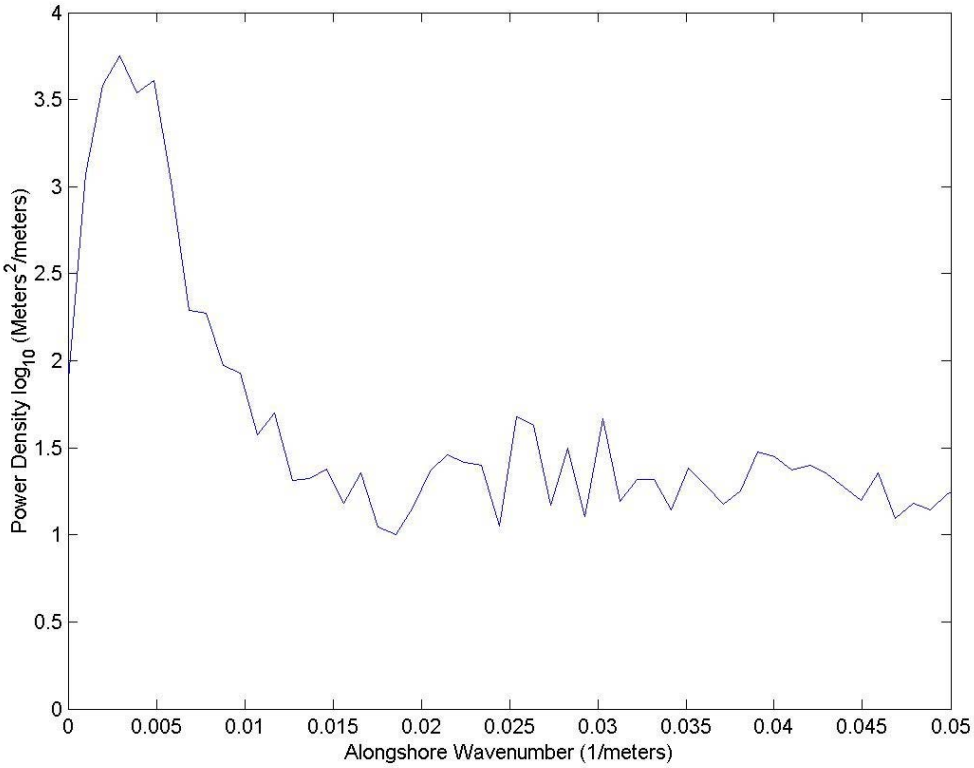

Figure 14. Wavenumber spectrum for the 1997 LIDAR survey of the Southern Monterey Bay shoreline. Alongshore wavenumber peaks correspond to cusp spacing 200-340m.

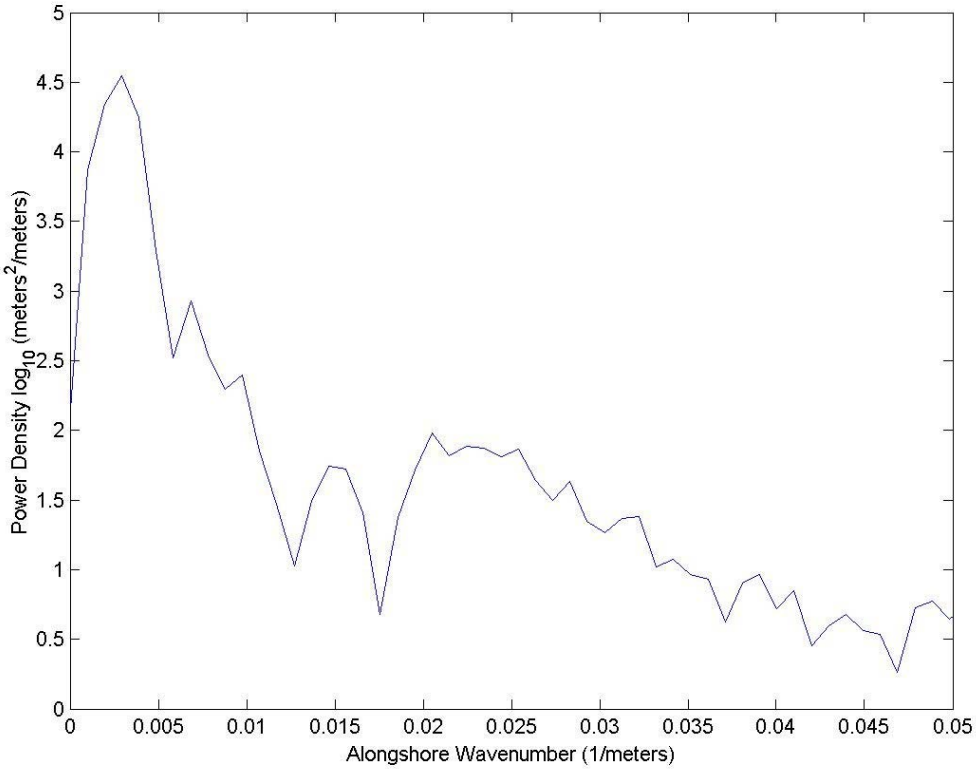

Figure 15. Wavenumber spectrum for the 1998 LIDAR survey of the Southern Monterey Bay shoreline. The peak at $K_y \cong 0.003(1/m)$ corresponds to a cusp spacing of $\lambda_c \cong 340m$.

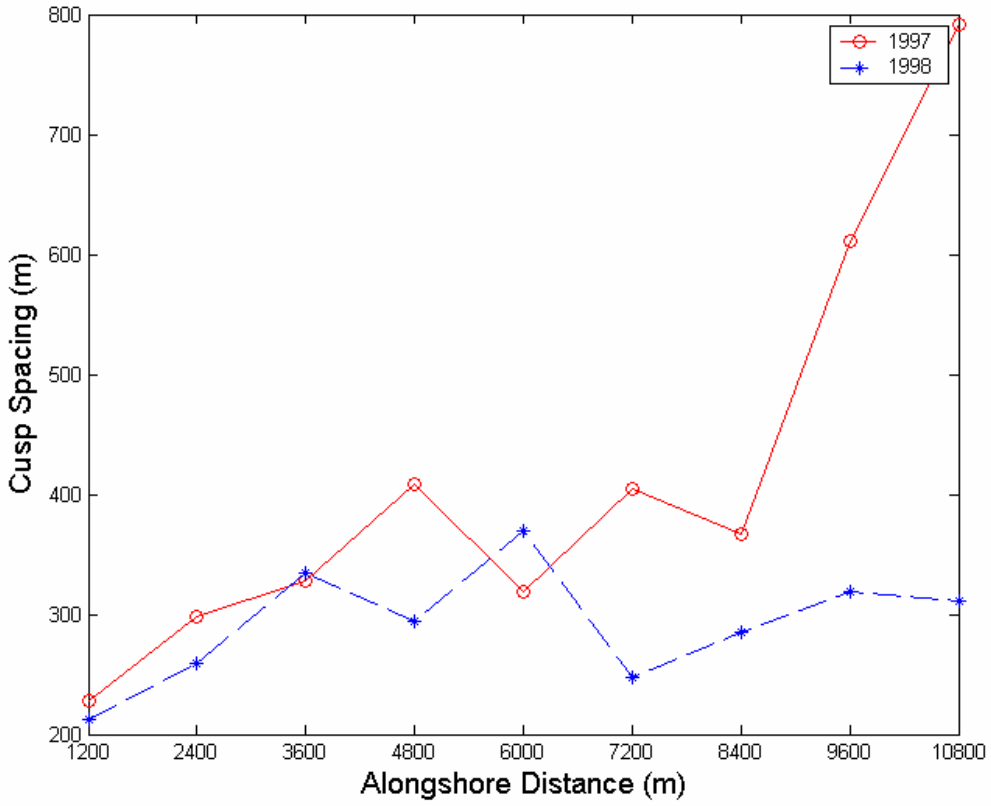

Figure 16. Cusp spacing, λ_c, averaged at discreet bins O(1km) from LIDAR surveys of Southern Monterey Bay for 1997 and 1998.

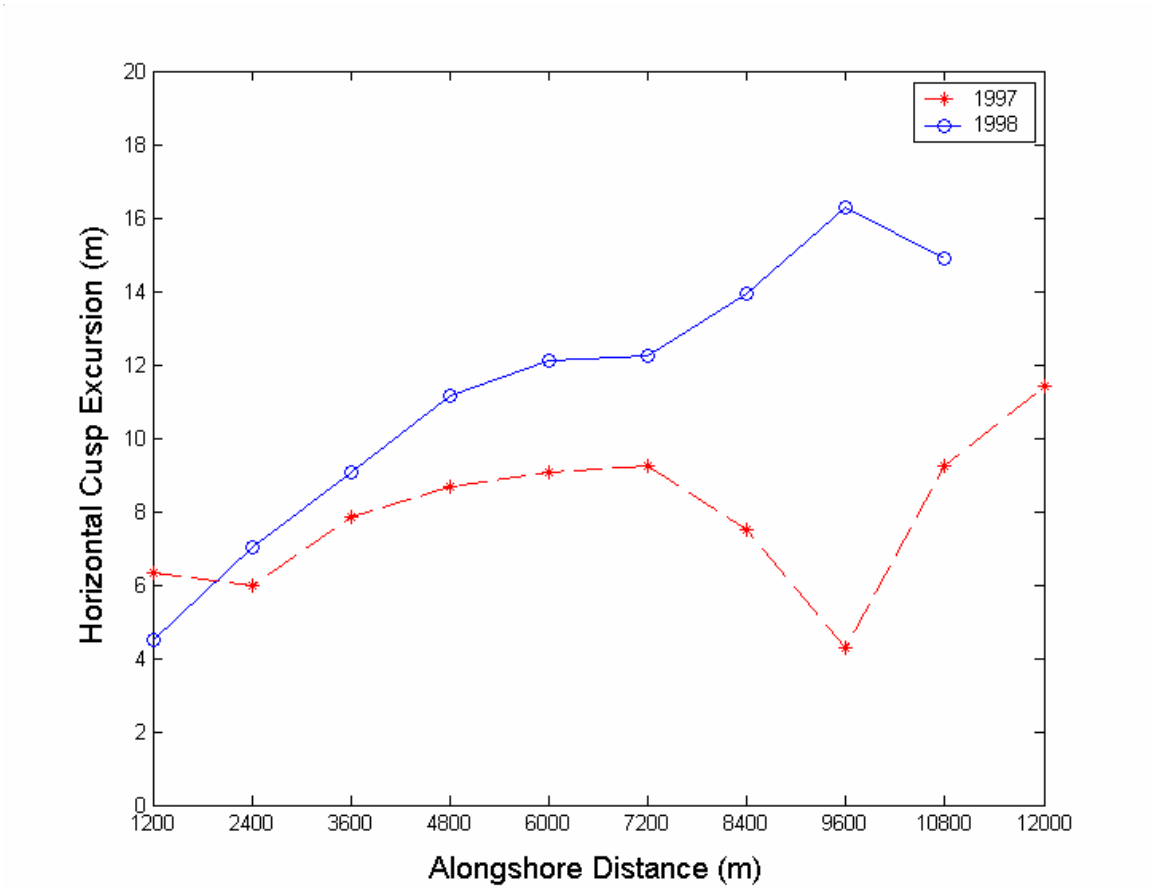

Figure 17. Horizontal Cusp Excursion of the Southern Monterey Bay. The values are averaged over bin sizes O(1km) and are derived from signal analysis of the 1997 and 1998 LIDAR surveys of the Monterey Bay.

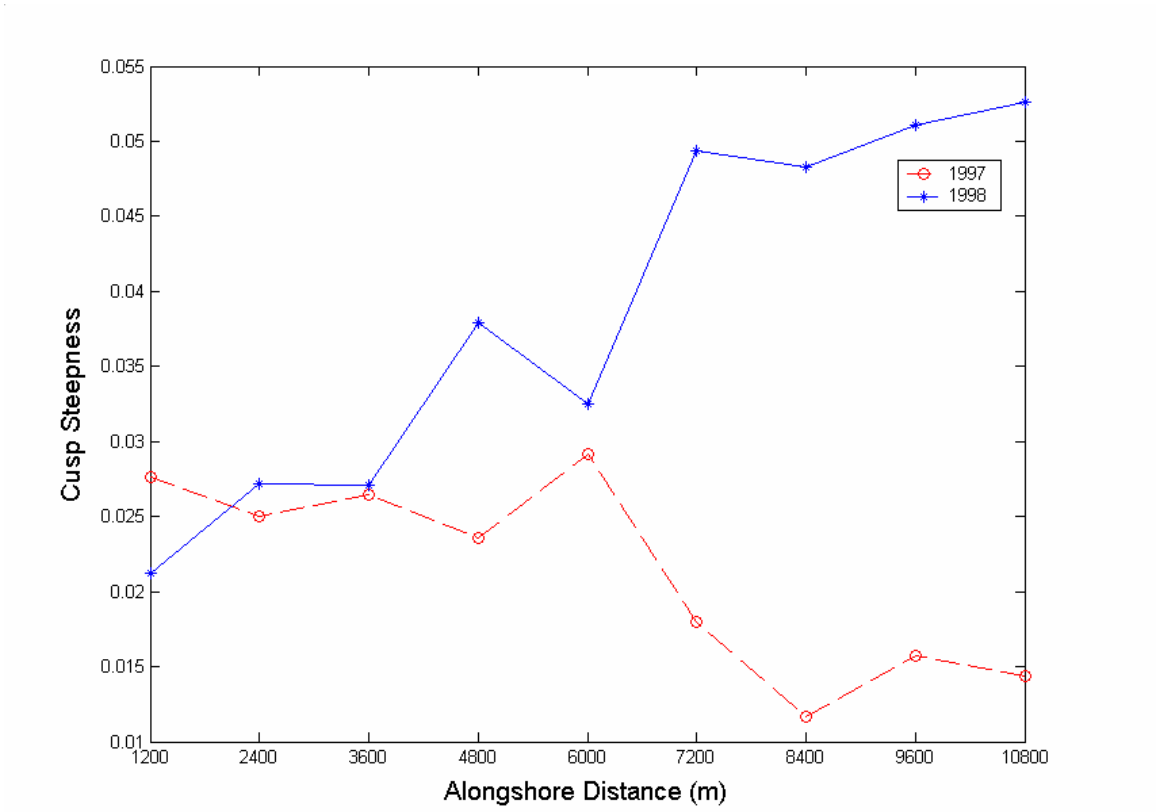

Figure 18. Cusp steepness, $\overline{\eta_c} / \lambda_c$, averaged over O(1km) bins for the length of the 1997 and 1998 LIDAR surveys of the Southern Monterey Bay.

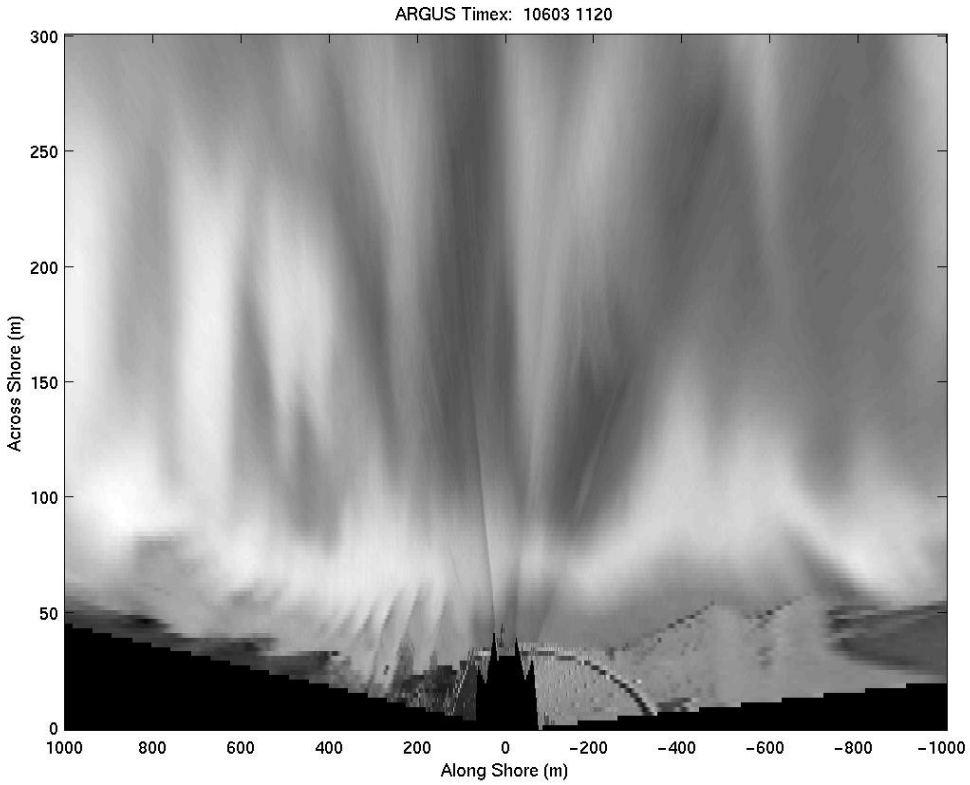

Figure 19. An Argus merged and rectified timex from the five camera array at Marina, Monterey Bay, CA from 06 January 2003, showing the cuspate shoreline and underlying bathymetry.

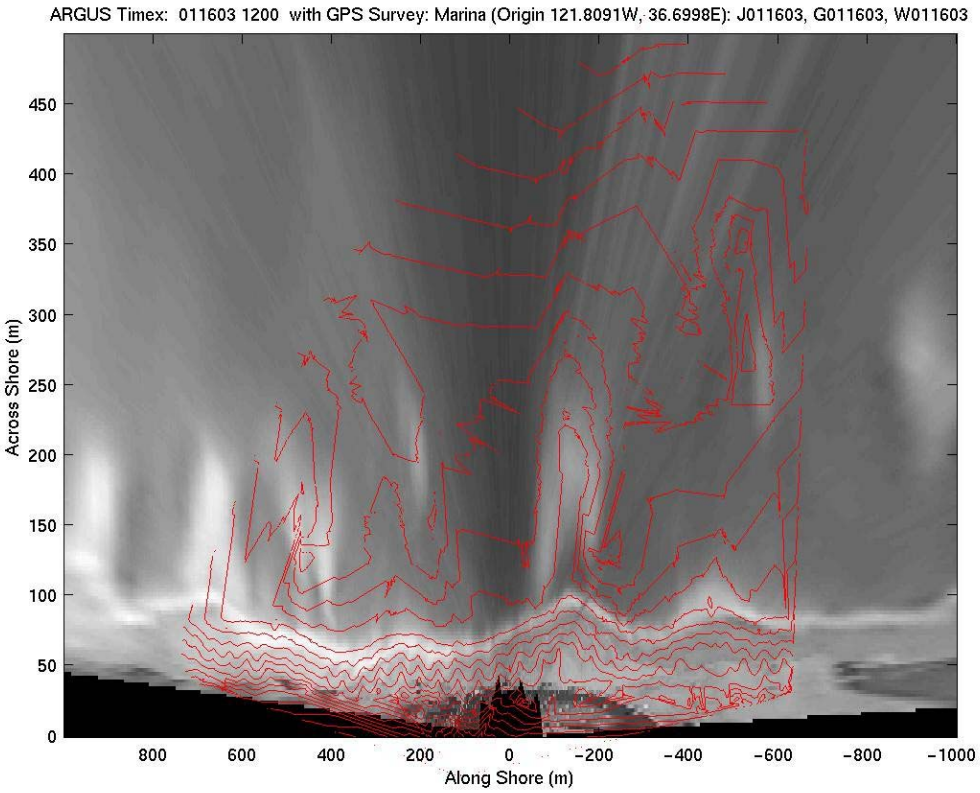

Figure 20. An Argus timex from 16 January, 2003 overlaid with contouring from the 16 January beach morphology surveying of Marina State Beach, Monterey Bay, CA. A well-defined rip channel is present in both surveys at $x = 0m$, though the alongshore swath width of the PWC limits validation of the cuspate features present in the timex.

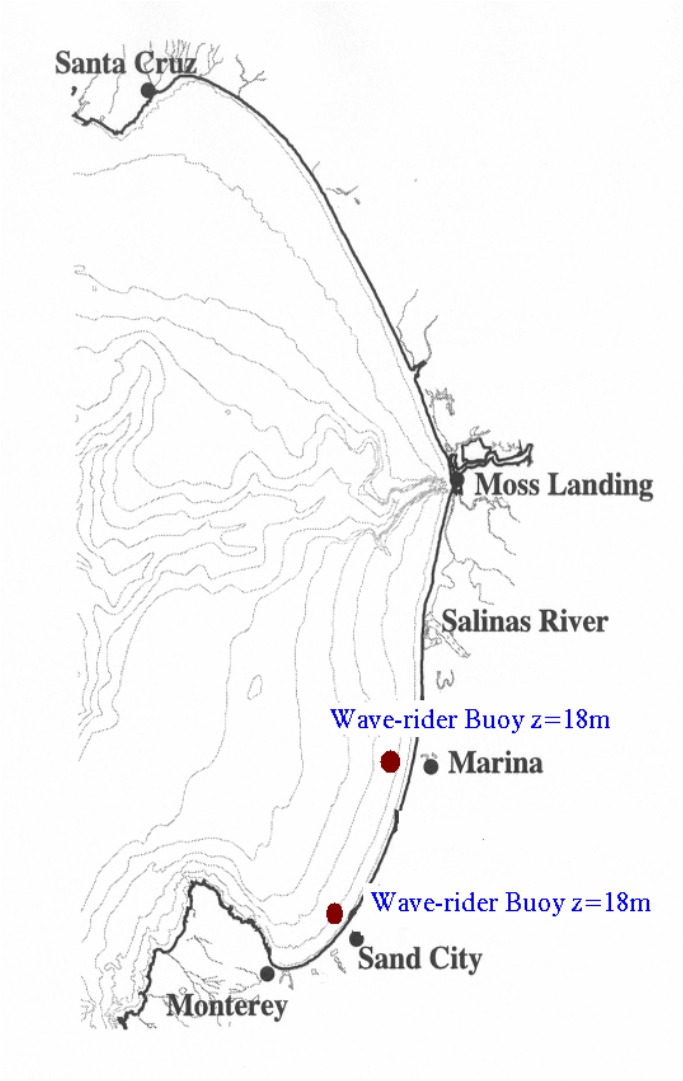

Figure 21. Location of the wave climate sensors in the Southern Monterey Bay.

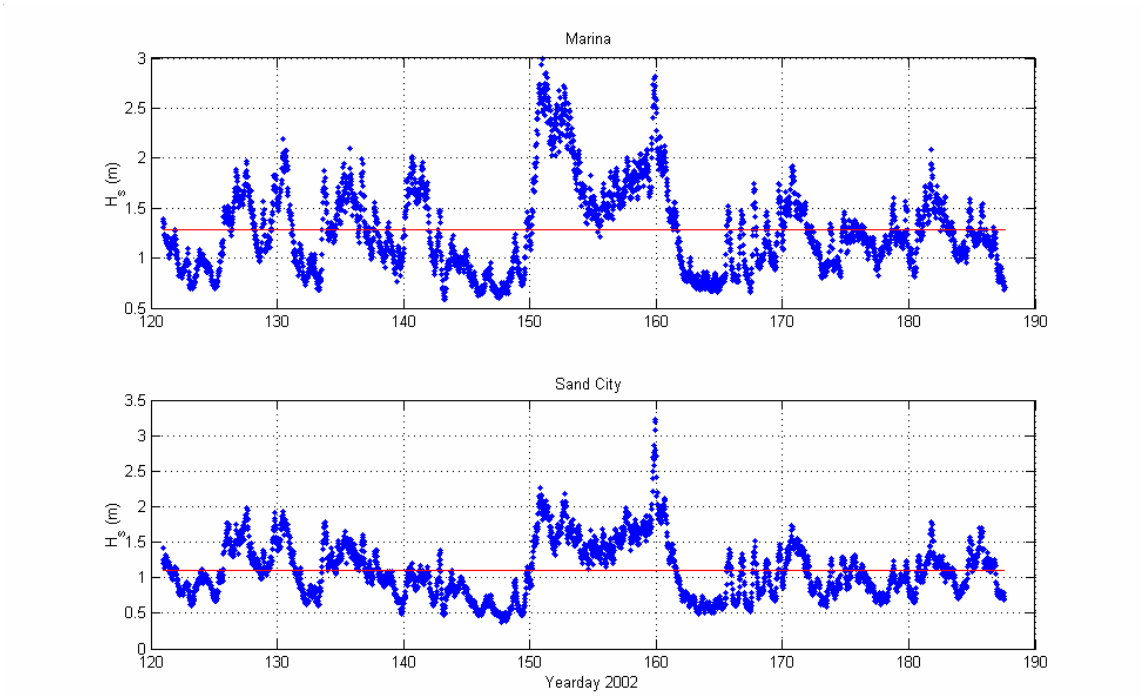

Figure 22. Significant wave height (m) plotted against yearday in 2002 from the directional wave buoys offshore of Marina and Sand City, Monterey Bay, USA. Mean values are shown in red.

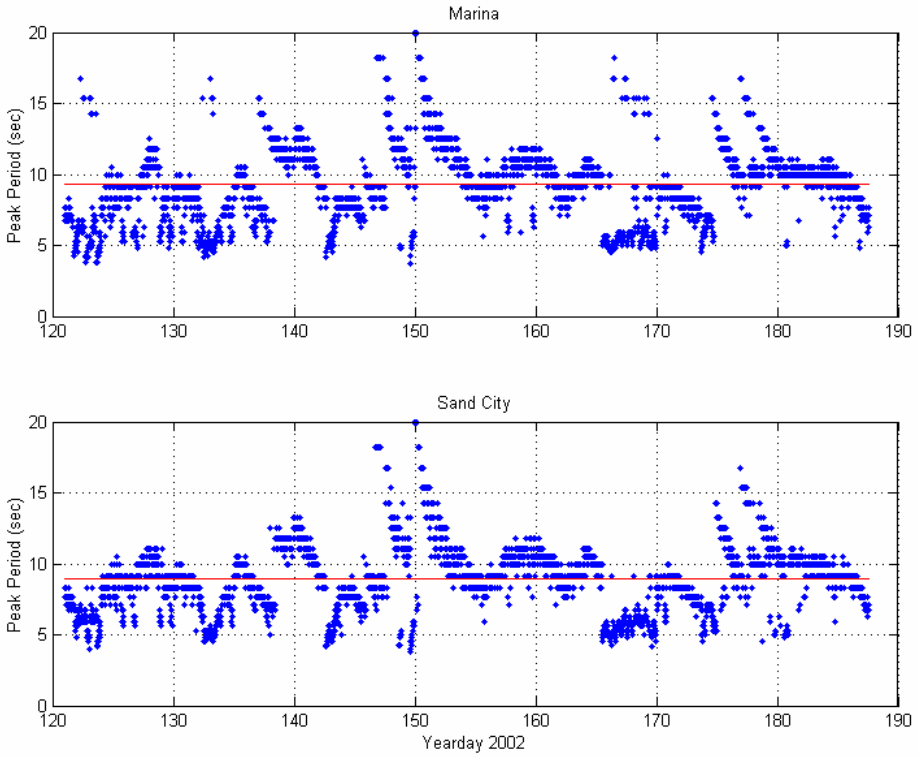

Figure 23. Peak period (sec) of incident wave trains plotted against yearday in 2002 from the directional wave buoys offshore of Marina and Sand City, Monterey Bay, USA. Mean values are shown in red.

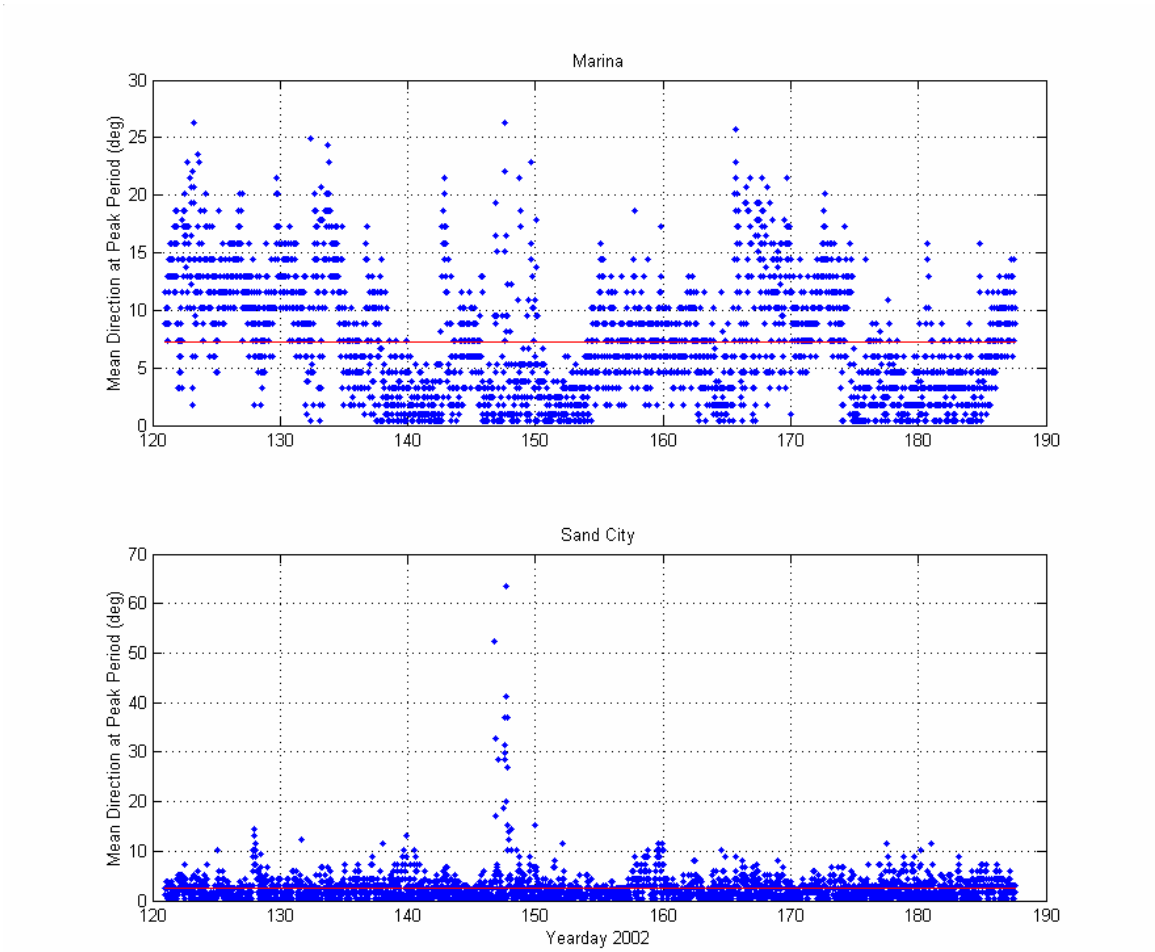

Figure 24. Mean direction (deg) of the incident wave trains at peak period plotted against yearday in 2002 from the directional wave buoys offshore of Marina and Sand City, Monterey Bay, USA. Mean values are shown in red.

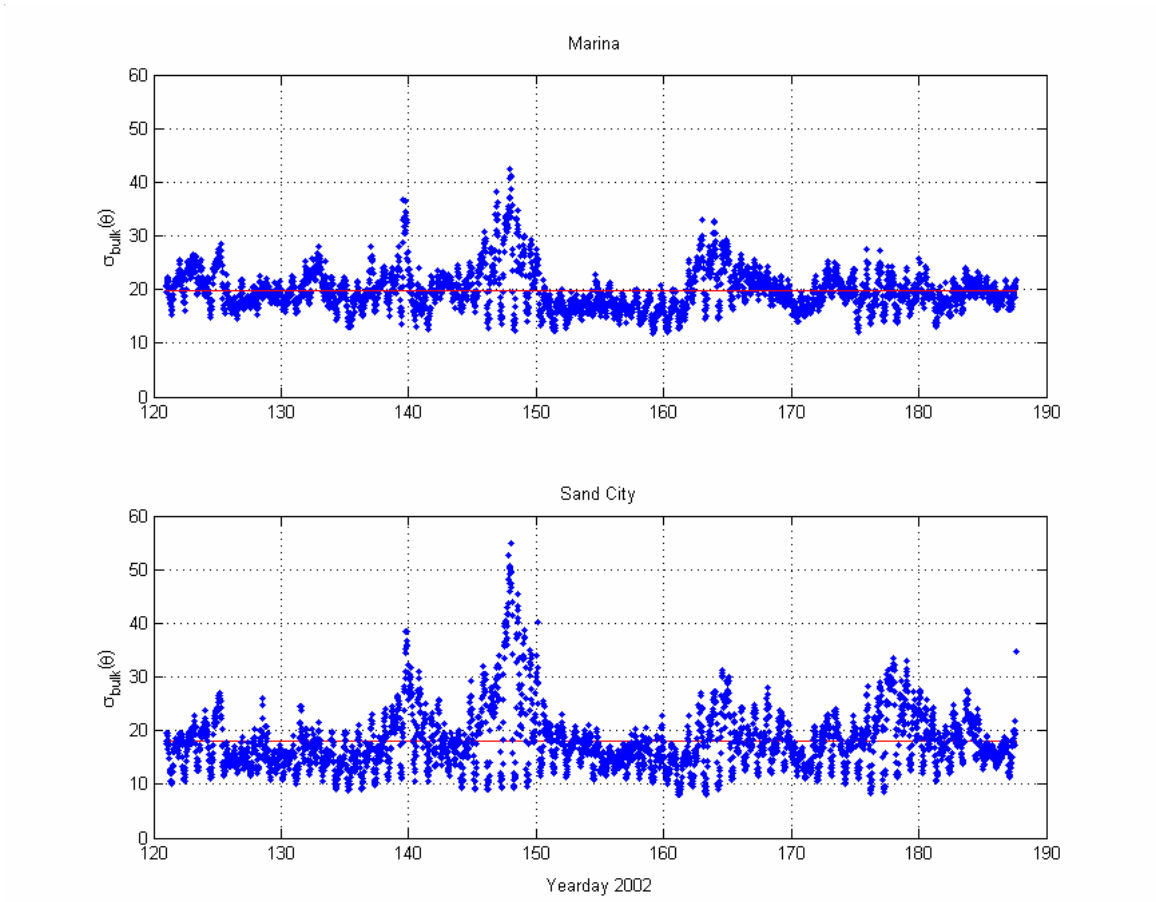

Figure 25. Bulk directional spreading, σ_{bulk}, plotted against yearday in 2002 from the moments of the directional wave buoys offshore of Marina and Sand City, Monterey, USA in 18m of depth. Mean values are shown in red.

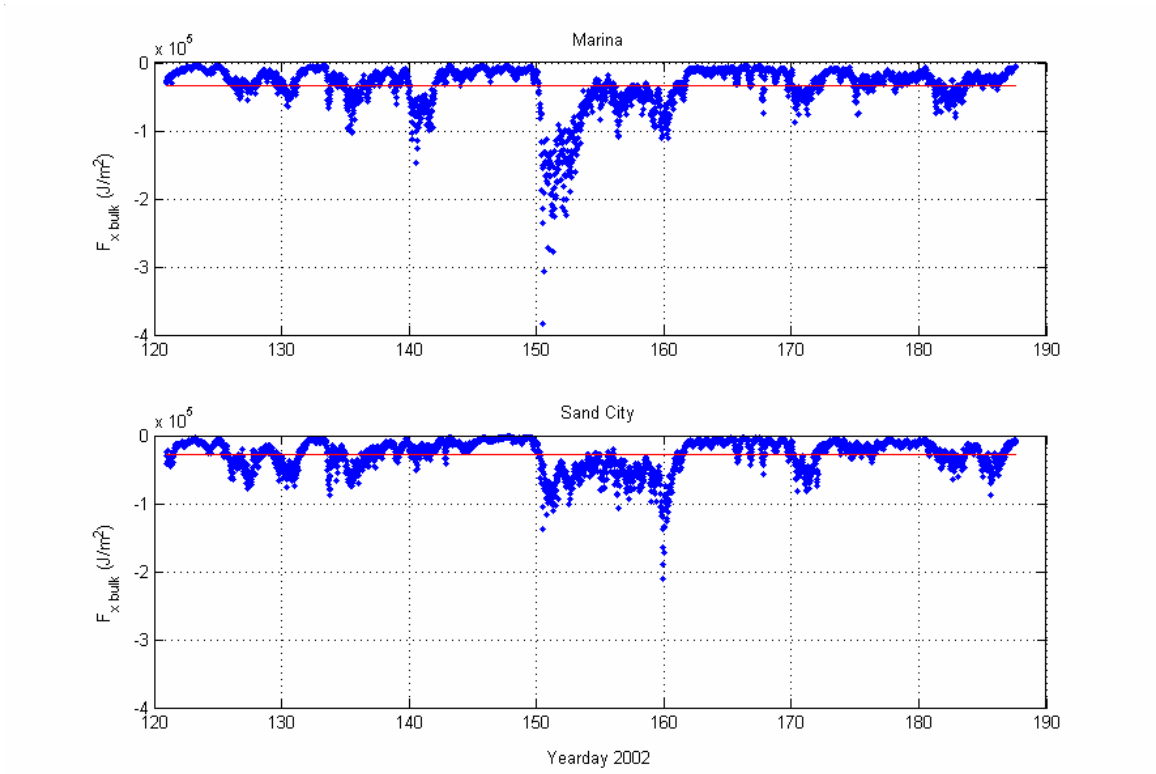

Figure 26. Cross-shore bulk energy flux plotted against yearday in 2002 from the directional wave buoys offshore of Marina and Sand City, Monterey Bay, USA. Mean values are shown in red. Onshore values are negative.

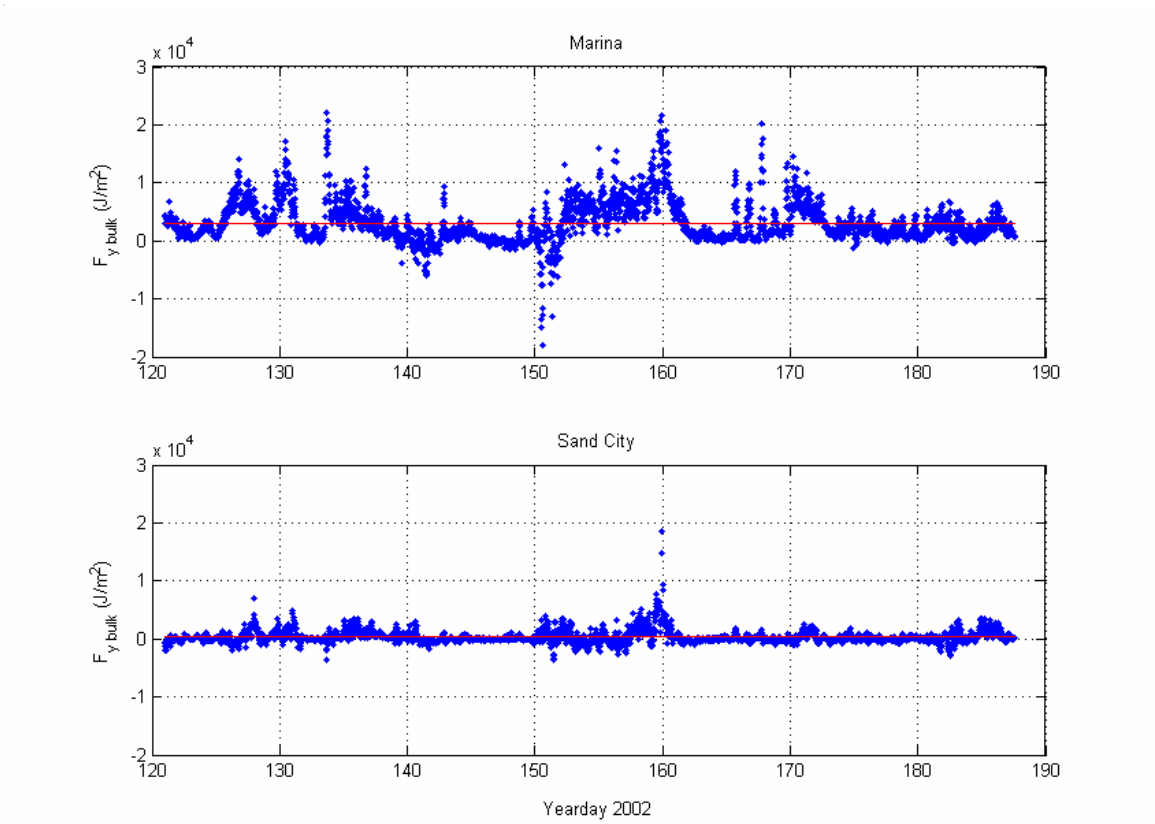

Figure 27. Alongshore bulk energy flux plotted against yearday in 2002 from the directional wave buoys offshore of Marina and Sand City, Monterey Bay, USA. Mean values are shown in red. Southward values are positive, indicating fluxes toward Del Monte Beach.

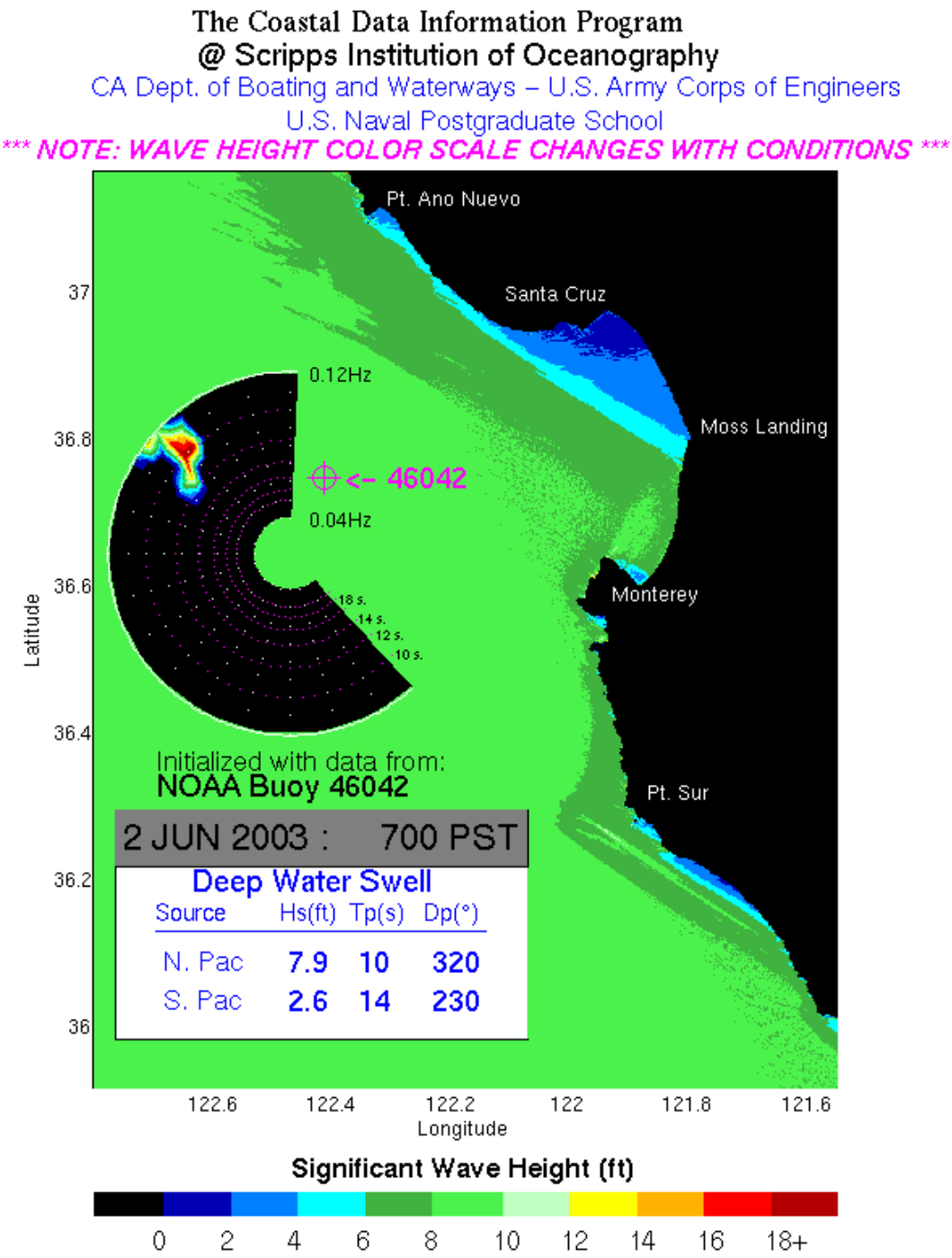

Figure 28. Output from O'Reilly's pure refraction wave model for the Monterey Bay. The model is initialized with directional spectra shown in the sub-graphic, indicating the directional distribution of the energy at various frequencies incident at NOAA buoy 46042. Significant wave height (feet) is color coded below the graph.

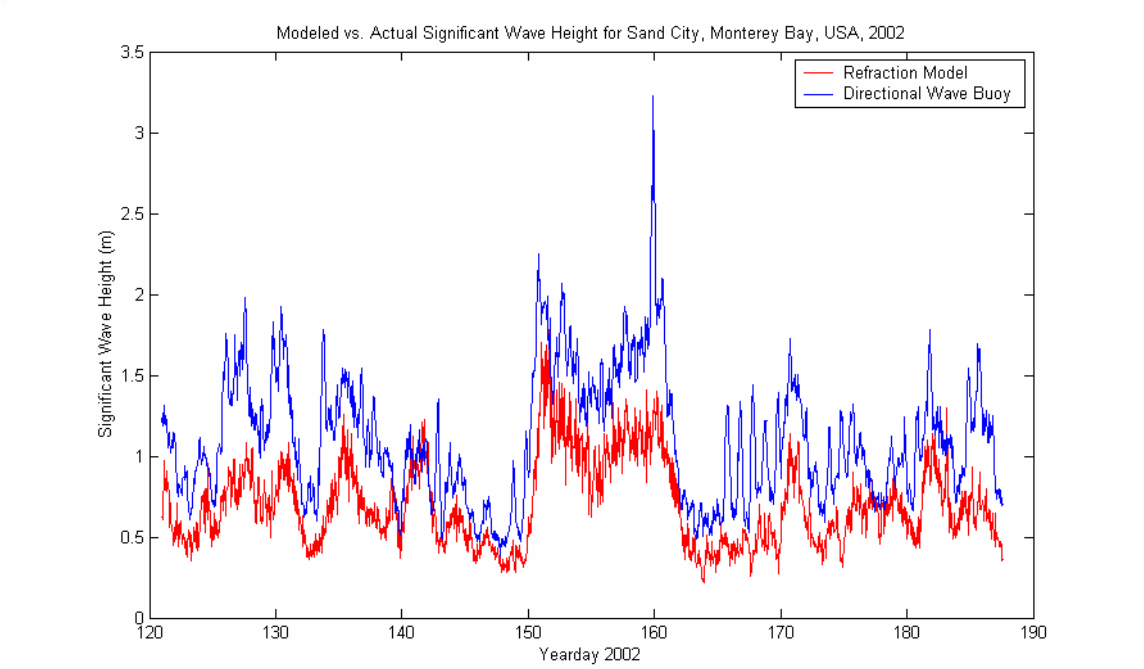

Figure 29. A comparison of the significant wave heights at Sand City in 2002, as generated by O'Reilly's refraction model and a directional wave-rider buoy located offshore in 18m of depth.

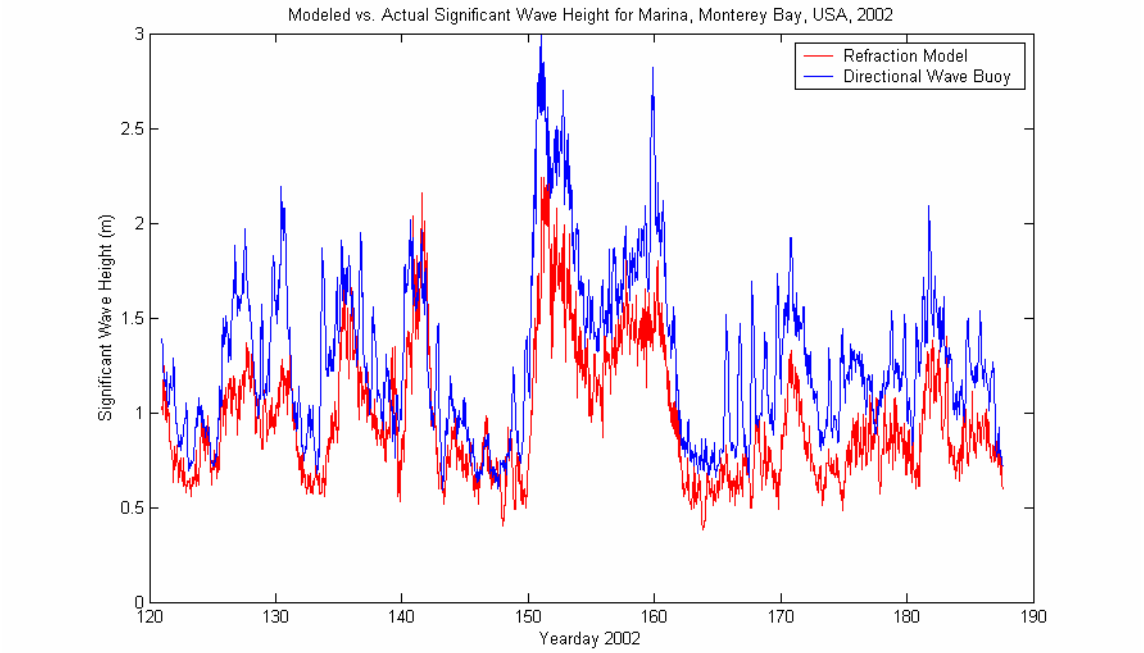

Figure 30. A comparison of the significant wave heights at Marina in 2002, as generated by O'Reilly's refraction model and a directional wave-rider buoy located offshore in 18m of depth.

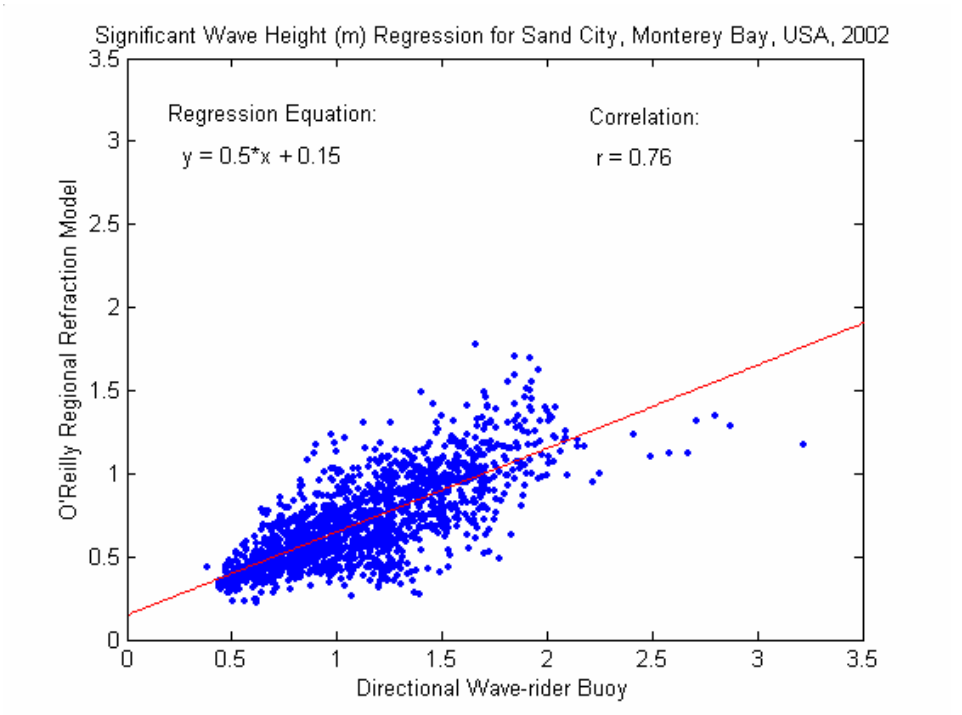

Figure 31. A linear regression of the H_s recorded by the Sand City wave buoy with O'Reilly's refraction model run at the same location and depth.

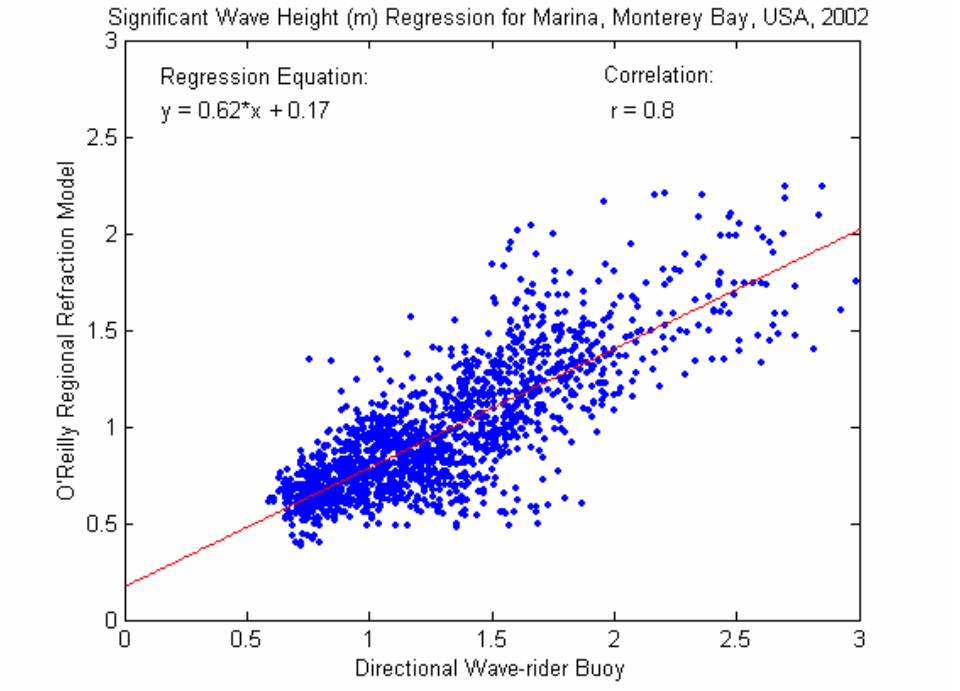

Figure 32. A linear regression of the H_s recorded by the Marina wave buoy with O'Reilly's refraction model run at the same location and depth.

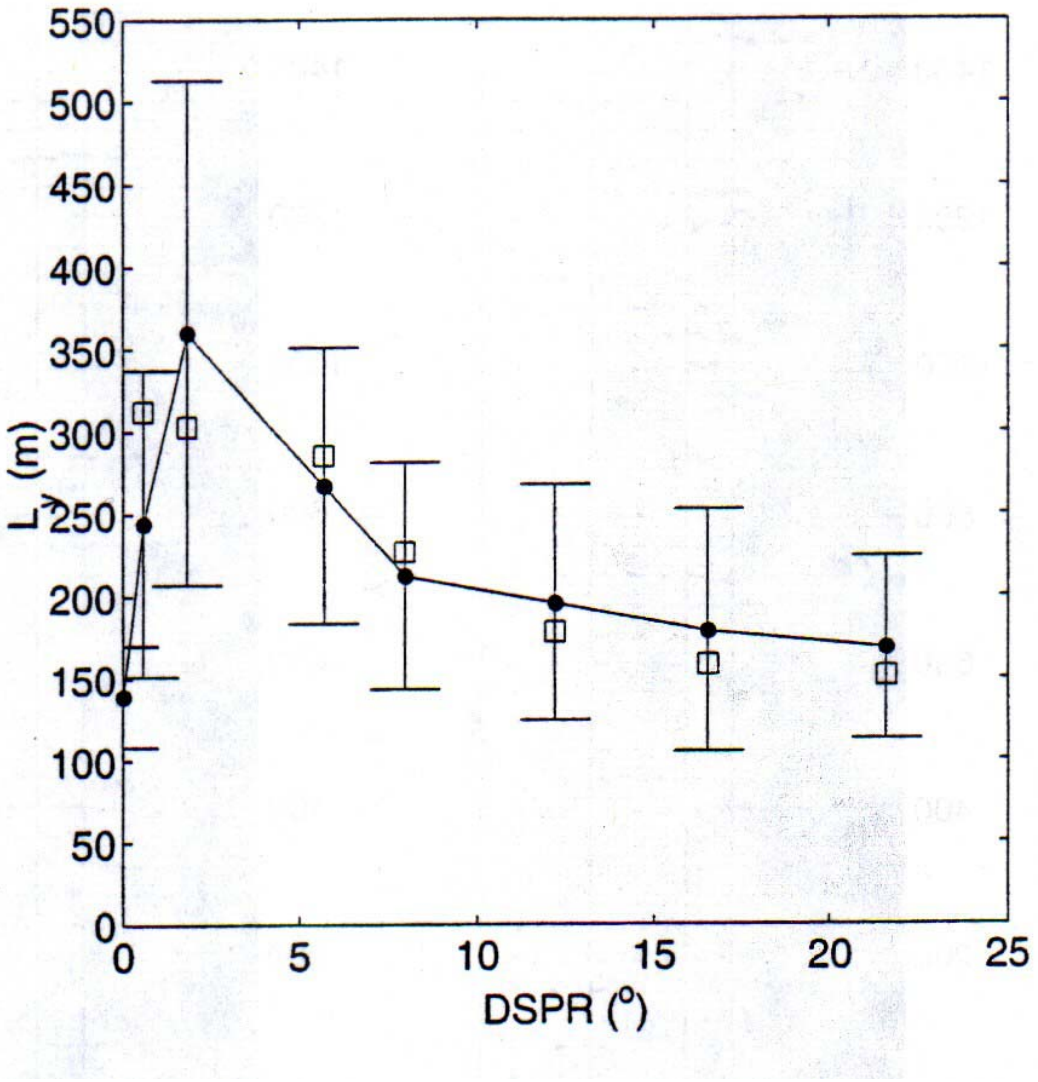

Figure 33. Alongshore wavelength, L_y, plotted against the directional spreading parameter, σ_{bulk}, as calcuated by the Delft 3-D morphodynamic model (Reniers *et al.* 2003). Model runs are for constant $H_s = 1m$ and $\theta_{mean} = 0^\circ$ and an initially longshore uniform barred beach. At $\sigma_{bulk} = 0^\circ$, the circulation is self-organized and a minimum L_y is predicted. Adding a small amount of directional spreading, $\sigma_{bulk} = 2^\circ$, made the beach quasi-forced and resulted in a maximum L_y. Further increases in σ_{bulk} resulted in a decrease in L_y.

THIS PAGE INTENTIONALLY LEFT BLANK

LIST OF REFERENCES

Abreu, M., A. Larraza, and E. Thornton, "Nonlinear Transformation of Directional Wave Spectra in Shallow Water," *J. of Geophys. Res.*, v. 97 (C10), 15579-15589, 1992.

Bowen, A. J., "Rip Currents, I: Theoretical Considerations," *J. of Geophys. Res.,* v. 74, pp. 5467-5478, 1969.

Bowen, A. J. and D. L. Inman, "Rip Currents, II: Laboratory and Field Observations," *J. of Geophys. Res.*, v.74, pp. 5479-5490, 1969.

Brock, J., C. W. Wright, A. H. Sallenger, W. Krabill, and R. N. Swift, "Basis and Methods of NASA Topographic Mapper LIDAR Surveys for Coastal Studies," *J. Coast. Res.*, v. 18, pp. 1-13, 2002.

Dalrymple, R.A., "A Mechanism for Rip Current Generation on an Open Coast," *J. Geophys. Res.*, v. 80, pp. 3485-3487, 1975.

Folwer, R. E. and R. A. Dalrymple, "Wave Group Forced Nearshore Circulation," Proceedings of the 22nd International Conference on Coastal Engineering, pp. 729-742, Am. Soc. of Civ. Eng., Delft, 1990.

Herbers, T. H. C., S. Elgar, and R. T. Guza, "Directional Spreading of Waves in the Nearshore," J. Geophys. Res., v. 104, pp. 7683-7693, 1999.

Holland, K. T., R. A. Holman, T. C. Lipmann, J. Stanley and N. Plant, "Practical Use of Video Imagery in Nearshore Oceanographic Field Studies," IEEE J. of Oceanographic Eng., v. 22 (1), pp. 81-92, 1997.

Holman, R. A. and T. C. Lippmann, "Remote Sensing of Nearshore Bar Systems—Making Morphology Visible," *Coast. Sediments*, v. 87, pp. 929-944, 1987.

Huntley, D. A. and Short, A. D., "On the Spacing Between Observed Rip Currents," *Coastal Eng.*, v. 17 (3-4), pp. 211-225, 1992.

Komar, P. D., "Nearshore Cell Circulation and the Formation of Giant Cusps," *Geol. Soc. of America Bulletin*, v. 82, pp. 2643-2650, 1971.

Komar, P. D., and W. G. McDougal, "Coastal Erosion and Engineering Structures: The Oregon Experience," *J. Coast. Res.*, v. 4, pp. 77-92, 1988.

Komar, P. D., *Beach Processes and Sedimentation,* pp. 429, Prentice-Hall, 1998.

Konicki, K. M., and R. A. Holman, "The Statistics and Kinematics of Transverse Sand Bars on an Open Coast," *Marine Geology*, v. 169, pp. 69-101, 2000.

List, J. and Farris, A., "Large-scale Shoreline Response to Storms and Fair Weather," *Coast.* Sediments '99, pp. 1324-1338, 1999.

Longuet-Higgins, M. S. and D. W. Parkin, "Sea Waves and Beach Cusps," *Geographical J.*, v. 128, pp. 194-201, 1962.

Longuet-Higgins, M. S., D. E. Cartwright and N. D. Smith, "Observations of the Directional Distribution in Ocean Wave Spectra," *Oc. Wave Spectra*, Prentice-Hall, pp. 111-136, 1963.

Longuet-Higgins, M. S. and R. W. Stewart, "Radiation Stress in Water Waves; a

Physical Discussion with Applications," *Deep Sea Res.*, v.2, pp. 529-563, 1964.

MacMahan, J., "Hydrographic Surveying from a Personal Watercraft," *J. of Surveying Eng.*, v. 127 (1), pp. 12-24, 2001.

MacMahan, J., A. Reniers, E. B. Thornton, and T. P. Stanton, "Observations of Infragravity Waves and Rip Current Pulsations," *submitted to J. of Geophys. Res.,* 2003a.

MacMahan, J., E. B. Thornton, T. P. Stanton, and A. J. H. M. Reniers, "RIPEX-The Rip Currents on a Shore-Connected Shoal Beach," *submitted to Marine Geo.*, 2003b.

Mei, C. C. and P. L-F. Liu, "Effects of Topography on the Circulation in and Near the Surf Zone—Linear Theory," *Estuarine and Coastal Marine Science*, v. 5, pp. 25-37, 1976.

Munk, W. H. and M. A. Traylor, "Refraction of Ocean Waves: A Process Linking Underwater Topography to Beach Erosion," *J. of Geology*, v. 55 (1), pp. 1-26, 1947.

O'Reilly, W. C., and R. T. Guza, "Comparison of Spectral Refraction and Refraction-Diffraction Wave Models," *J. of Waterway, Port, Coastal, and Oc. Eng.,* v. 117 (3), pp. 199-215, 1991.

O'Reilly, W. C., and R. T. Guza, "Assimilating Coastal Wave Observations in Regional Swell Predictions. Part I: Inverse Methods," *J. of Phys. Oc.*, v. 28, pp. 679-691, 1998.

Ranasignhe, R., G. Symonds and Rob Holman, "Quantitative Characterization of Rip Dynamics via Video Imaging," *Coastal Sediments,* pp. 987-1001, 1999.

Ranasinghe, R., G. Symonds, K. Black and R. Holman, "Processes Governing Rip Spacing, Persistence, and Strength in a Swell Dominated, Microtidal Environment," *Proceedings from the 27th International. Conference on Coastal Eng.,* ASCE, pp. 454-467, 2001.

Reniers, A. D., D. Roelvink, and E. B. Thornton, "Morphodynamic Modeling of an Embayed Beach Under Wave Group Forcing," *accepted by J. Geophys. Res.*, 2003.

Revell, D. L., P. D. Komar, and A. H. Sallenger, Jr., "An Application of LIDAR to Analyses of El Nino Erosion in the Netarts Littoral Cell, Oregon," *J. Coast. Res.,* v. 18(4), pp. 792-801, 2002.

Sallenger, A. H., W. Krabill, J. Brock, R. Swift, S. Manizade, and H. Stockdon, "Sea-Cliff Erosion as a Function of Beach Changes and Extreme Wave Runup During the 1997-1998 El Nino," *Marine Geology,* v. 187, pp. 279-297, 2002.

Sallenger, A. H., W. Krabill, J. Brock, R. Swift, S. Manizade, and others, "Evaluation of Airborne Topographic LIDAR for Quantifying Beach Changes," *J. Coast. Res.,* v. 19(1), pp. 125-133, 2003.

Shepard, F. P., "Undertow, Riptides or Rip Currents," *Science*, v. 84, pp. 181-182, 1936.

Shepard, F. P., K. O. Emery, and E.C. La Fond, "Rip Currents: A Process of Geological Importance," *J. Geology*, v. 49, pp. 337-369, 1941.

Shepard, F. P., and D. L. Inman, "Nearshore Circulation Related to Bottom Topography and Wave Refraction," *Proc. of the 1st Con. of Coastal Eng.*, pp.50-59, 1950.

Short, A.D., “Rip Current Type, Spacing, and Persistence, Narrabeen Beach, Australia,” *Marine Geology*, v. 65, pp. 47-71, 1985.

Sonu, C. J., “Field Observation of Nearshore Circulation and Meandering Currents,” *J. Geophys. Res.*, v.77, pp.3232-3247, 1972.

Stockdon, H. F. and R. A. Holman, “”Estimation of Wave Phase Speed and Nearshore Bathymetry from Video Imagery,” *J. Geophys. Res.*, v. 105(c9), pp. 22015-22033, 2000.

Thornton, E. B., L. A. Egley, A. Sallenger, and R. Parsons, “Erosion in Southern Monterey Bay During the 1997-98 El Nino,” *Proceedings of Coastal Sediments ’03*, 10 pgs, 2003.

INITIAL DISTRIBUTION LIST

1. Defense Technical Information Center
   Ft. Belvoir, Virginia

2. Dudley Knox Library
   Naval Postgraduate School
   Monterey, California

3. Dr. Mary Batteen
   Chairman
   Department of Oceanography
   Naval Postgraduate School
   Monterey California

4. Dr. Edward Thornton
   Department of Oceanography
   Naval Postgraduate School
   Monterey, CA

5. Professor Timothy Stanton
   Department of Oceanography
   Naval Postgraduate School
   Monterey, CA

6. ENS Robert D. Holt, USNR
   USS PORT ROYAL (CG73)
   Pearl Harbor, HI

7. Dr. Ad T. Reniers
   Department of Oceanography
   Naval Postgraduate School
   Monterey, CA

8. Dr. Jamie MacMahan
   Department of Oceanography
   Naval Postgraduate School
   Monterey, CA

9. Mr. Mark D. Orzech
   Department of Oceanography
   Naval Postgraduate School
   Monterey, CA

10. Mr. Robert M. Wyland
Department of Oceanography
Naval Postgraduate School
Monterey, CA

11. Dr. William C. O'Reilly
Department of Oceanography
Naval Postgraduate School
Monterey, CA

12. Mr. James Stockel
Department of Oceanography
Naval Postgraduate School
Monterey, CA

13. Mr. Paul Jessen
Department of Oceanography
Naval Postgraduate School
Monterey, CA

14. CDR John Joseph, USN
Department of Oceanography
Naval Postgraduate School
Monterey, CA

15. RADM John Pearson, USN (Ret.)
Undersea Warfare
Naval Postgraduate School
Monterey, CA

16. Dr. Mario Vieira
Department of Oceanography
United States Naval Academy
Annapolis, MD

17. Dr. Todd Sikora
Department of Oceanography
United States Naval Academy
Annapolis, MD

18. CDR Henry Jones, USN
Department of Oceanography
United States Naval Academy
Annapolis, MD

19. CDR Thomas Holt, USN (Ret.)
Vice President of Human Resources
Trajen Corporation
Bryan, TX

20. Dr. Kai Chang
Department of Electrical Engineering
Texas A&M University
College Station, TX

21. Dr. Victor Willson
Department of Educational Psychology
Texas A&M University
College Station, TX